

CKDMIP: CKD tool performance evaluation

May 3, 2020

CKD tool: **ecCKD version 0.5** Spectral domain: **Longwave** Application: **Limited-Area NWP** Evaluation dataset: **Evaluation-1**

Contents

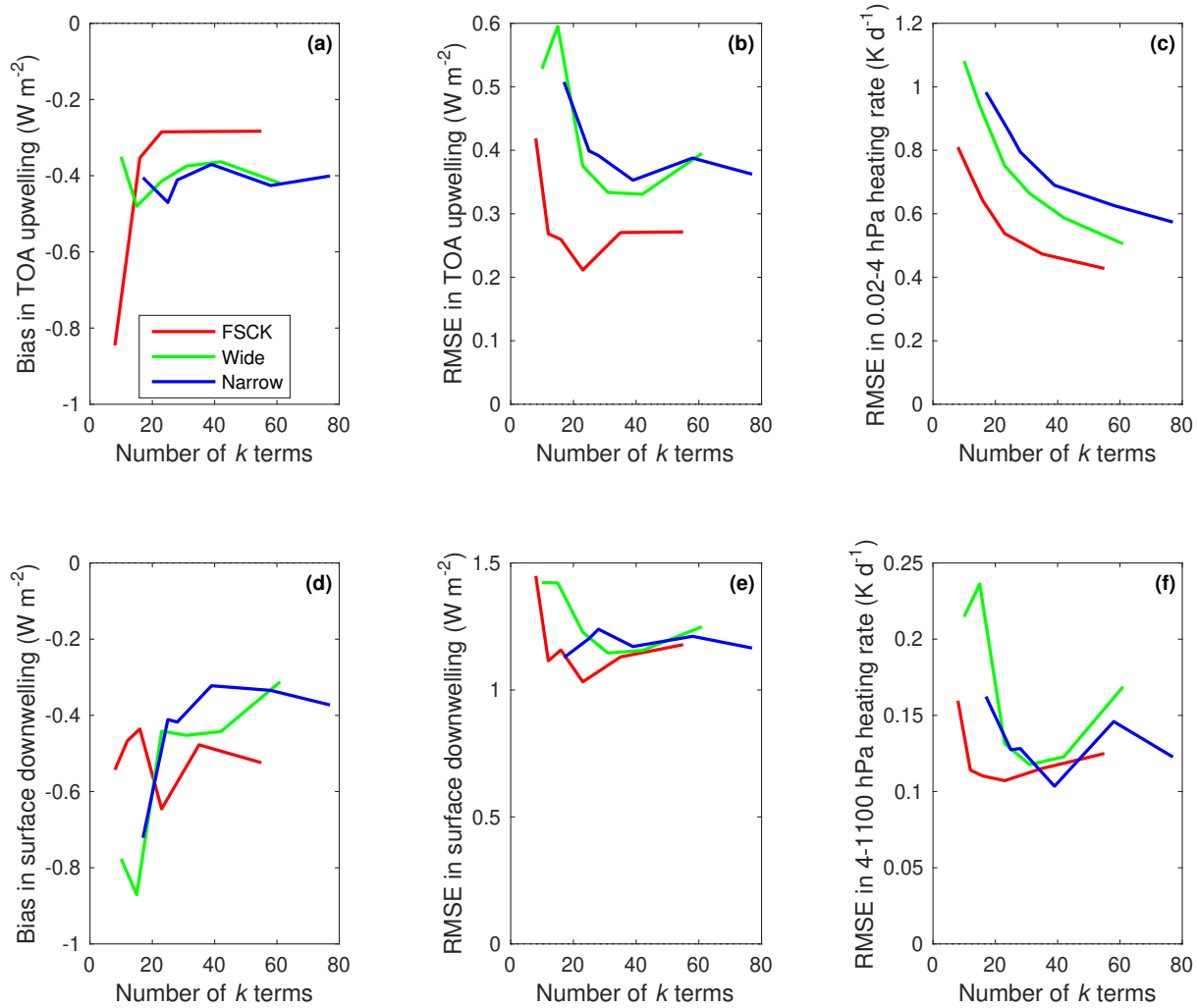
Model 1:	ecCKD limited-area-nwp-fsck-8	3
Model 2:	ecCKD limited-area-nwp-fsck-12	4
Model 3:	ecCKD limited-area-nwp-fsck-16	5
Model 4:	ecCKD limited-area-nwp-fsck-23	6
Model 5:	ecCKD limited-area-nwp-fsck-35	7
Model 6:	ecCKD limited-area-nwp-fsck-55	8
Model 7:	ecCKD limited-area-nwp-wide-10	9
Model 8:	ecCKD limited-area-nwp-wide-15	11
Model 9:	ecCKD limited-area-nwp-wide-23	13
Model 10:	ecCKD limited-area-nwp-wide-31	15
Model 11:	ecCKD limited-area-nwp-wide-42	17
Model 12:	ecCKD limited-area-nwp-wide-61	19
Model 13:	ecCKD limited-area-nwp-narrow-17	21
Model 14:	ecCKD limited-area-nwp-narrow-25	23
Model 15:	ecCKD limited-area-nwp-narrow-28	25
Model 16:	ecCKD limited-area-nwp-narrow-39	27
Model 17:	ecCKD limited-area-nwp-narrow-58	29
Model 18:	ecCKD limited-area-nwp-narrow-77	31

Overview

This automatically generated document contains an evaluation of the performance of ecCKD for generating longwave correlated k -distribution (CKD) gas-optics models targeting the application *Limited-Area NWP*: atmospheric heating rates are required to a minimum pressure of 4 hPa, and evaluation is performed for present-day greenhouse gas concentrations. The evaluation dataset is *Evaluation-1* from the Correlated K-Distribution Model Intercomparison Project (CKDMIP)¹. Longwave radiative transfer is performed using four angles per hemisphere.

¹<https://confluence.ecmwf.int/display/CKDMIP>

The ecCKD tool has been used to generate CKD models with the following band structure(s): *fsck* (one full-spectrum band), *wide* (5 bands) and *narrow* (13 bands). For each band structure, a number of CKD models have been generated, characterized by the total number of k terms (also known as g points).



Biases and root-mean-squared errors (RMSE) in top-of-atmosphere (TOA) upwelling irradiance and surface downwelling irradiance, and RMSE in heating rate for two pressure ranges, for the various band structures as a function of the total number of k terms. It was computed from the “present-day” CKDMIP scenario.

Model 1: ecCKD limited-area-nwp-fsck-8

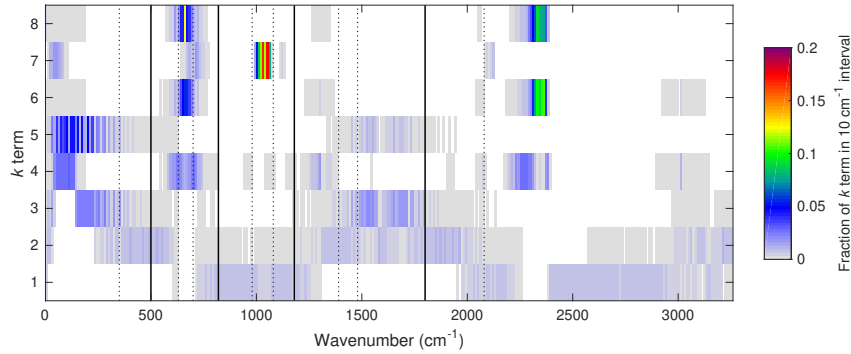
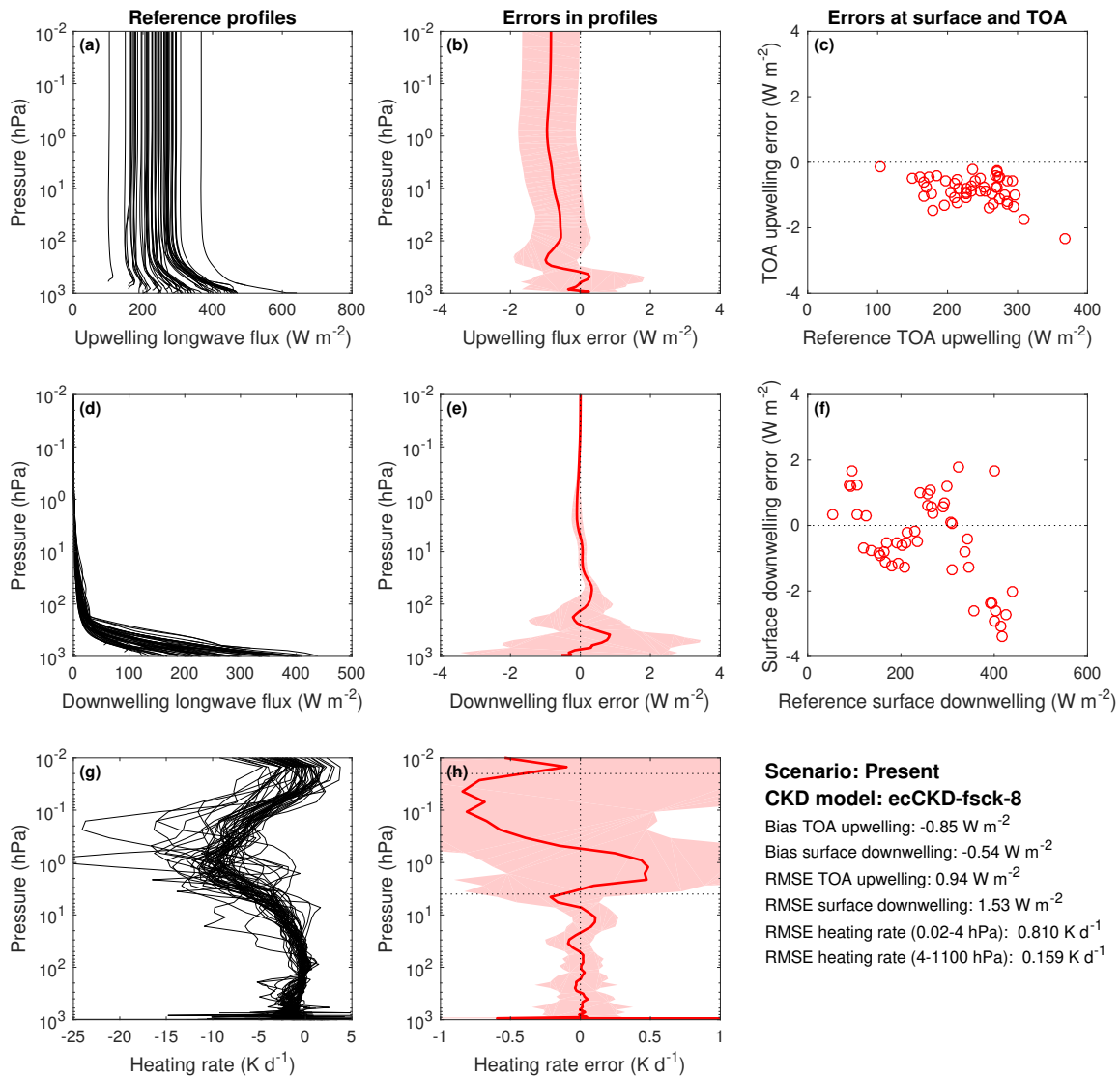


Illustration of the parts of the longwave spectrum that contribute to each k term of the limited-area-nwp-fsck-8 model.



Evaluation of the limited-area-nwp-fsck-8 CKD model for the “present-day” CKDMIP scenario. The left three panels show the irradiances and heating rates from the reference line-by-line calculations. The red lines in the middle three panels show the corresponding bias in these quantities from the CKD model. The shaded regions encompass 95% of the instantaneous errors. Panels c and f depict instantaneous errors in upwelling TOA and downwelling surface irradiances. Error metrics are provided in the lower right.

Model 2: ecCKD limited-area-nwp-fsck-12

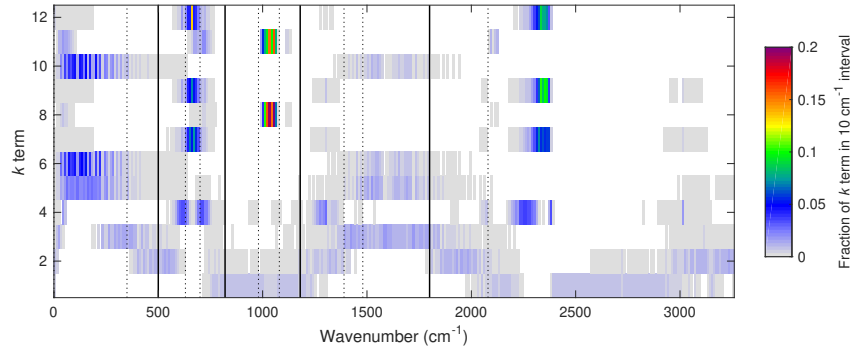
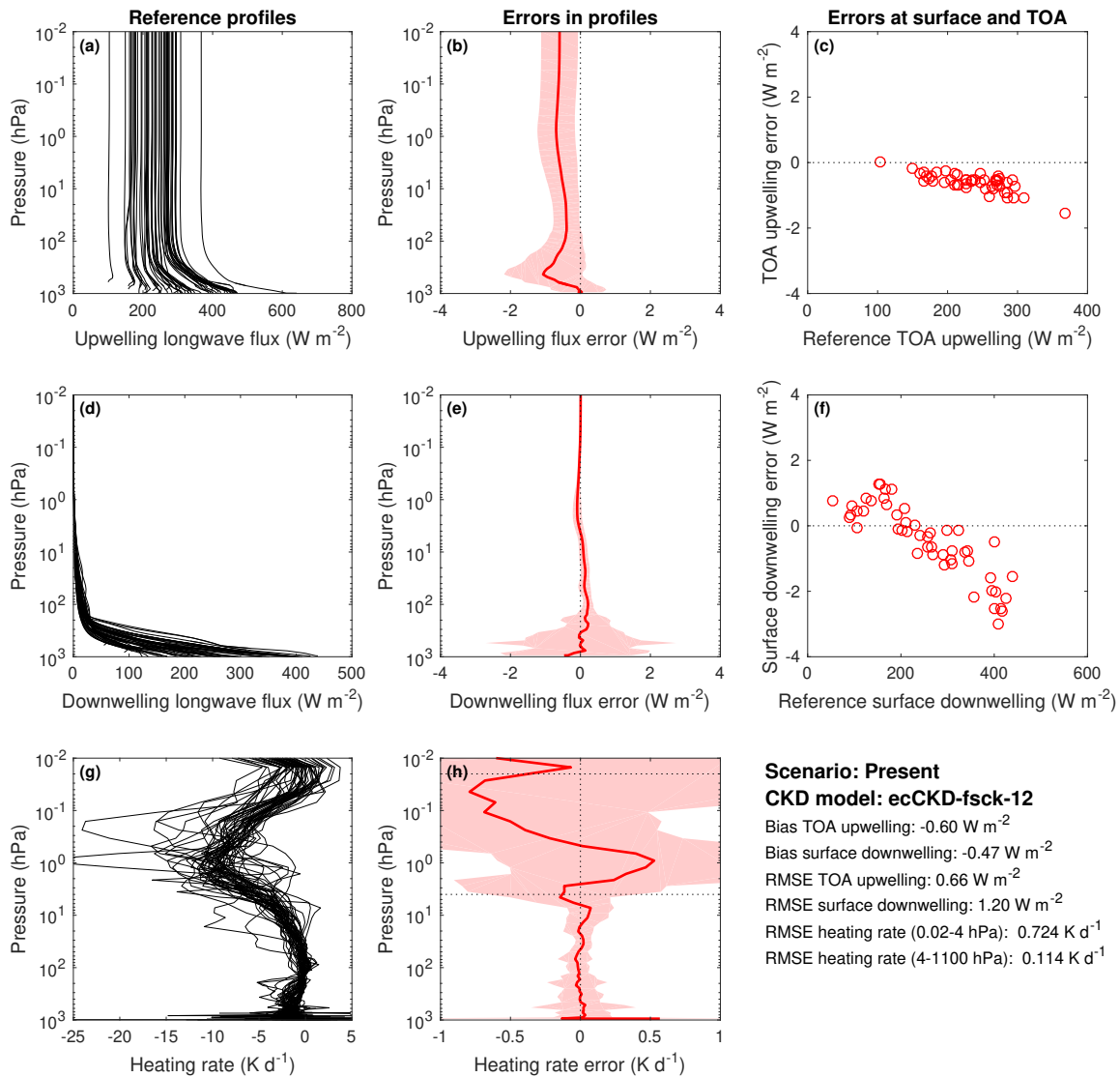


Illustration of the parts of the longwave spectrum that contribute to each k term of the limited-area-nwp-fsck-12 model.



Evaluation of the limited-area-nwp-fsck-12 CKD model for the “present-day” CKDMIP scenario. The left three panels show the irradiances and heating rates from the reference line-by-line calculations. The red lines in the middle three panels show the corresponding bias in these quantities from the CKD model. The shaded regions encompass 95% of the instantaneous errors. Panels c and f depict instantaneous errors in upwelling TOA and downwelling surface irradiances. Error metrics are provided in the lower right.

Model 3: ecCKD limited-area-nwp-fsck-16

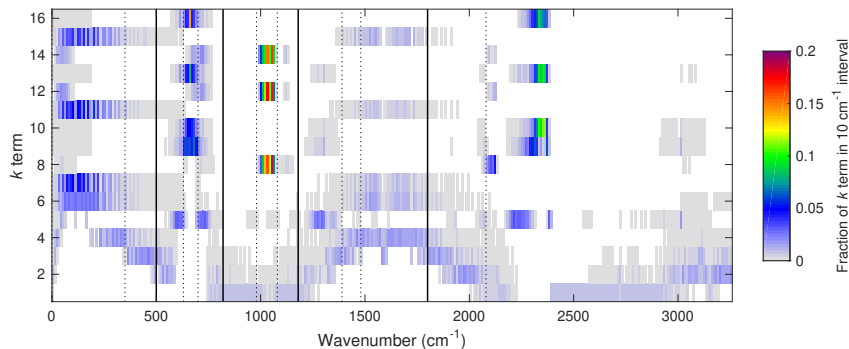
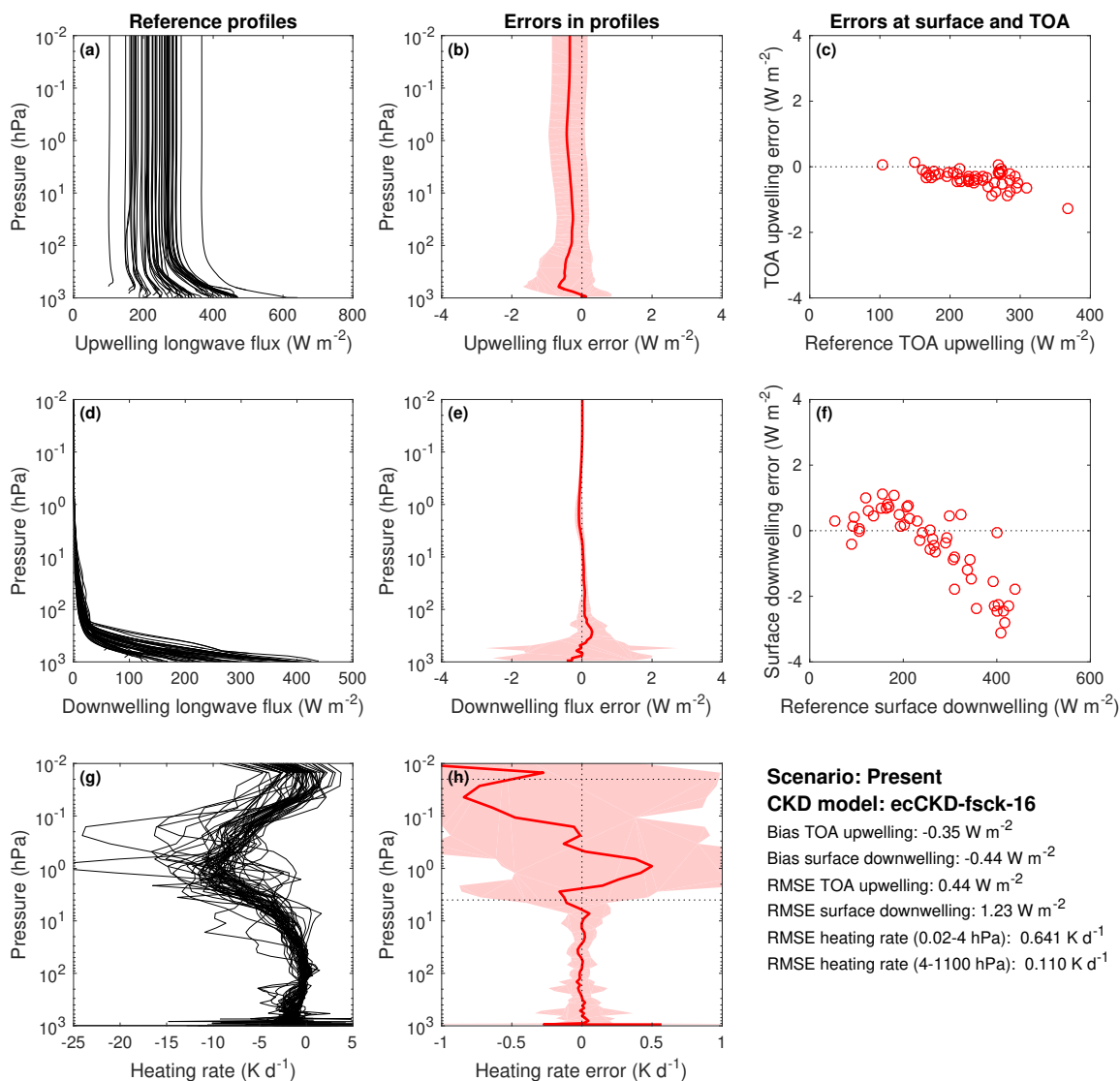


Illustration of the parts of the longwave spectrum that contribute to each k term of the limited-area-nwp-fsck-16 model.



Evaluation of the limited-area-nwp-fsck-16 CKD model for the “present-day” CKDMIP scenario. The left three panels show the irradiances and heating rates from the reference line-by-line calculations. The red lines in the middle three panels show the corresponding bias in these quantities from the CKD model. The shaded regions encompass 95% of the instantaneous errors. Panels c and f depict instantaneous errors in upwelling TOA and downwelling surface irradiances. Error metrics are provided in the lower right.

Model 4: ecCKD limited-area-nwp-fsck-23

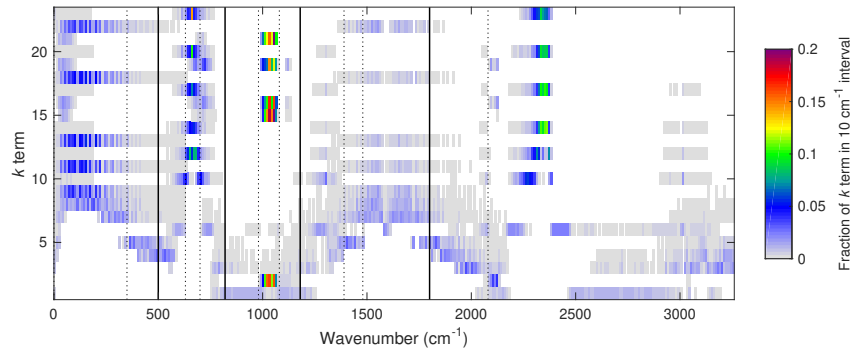
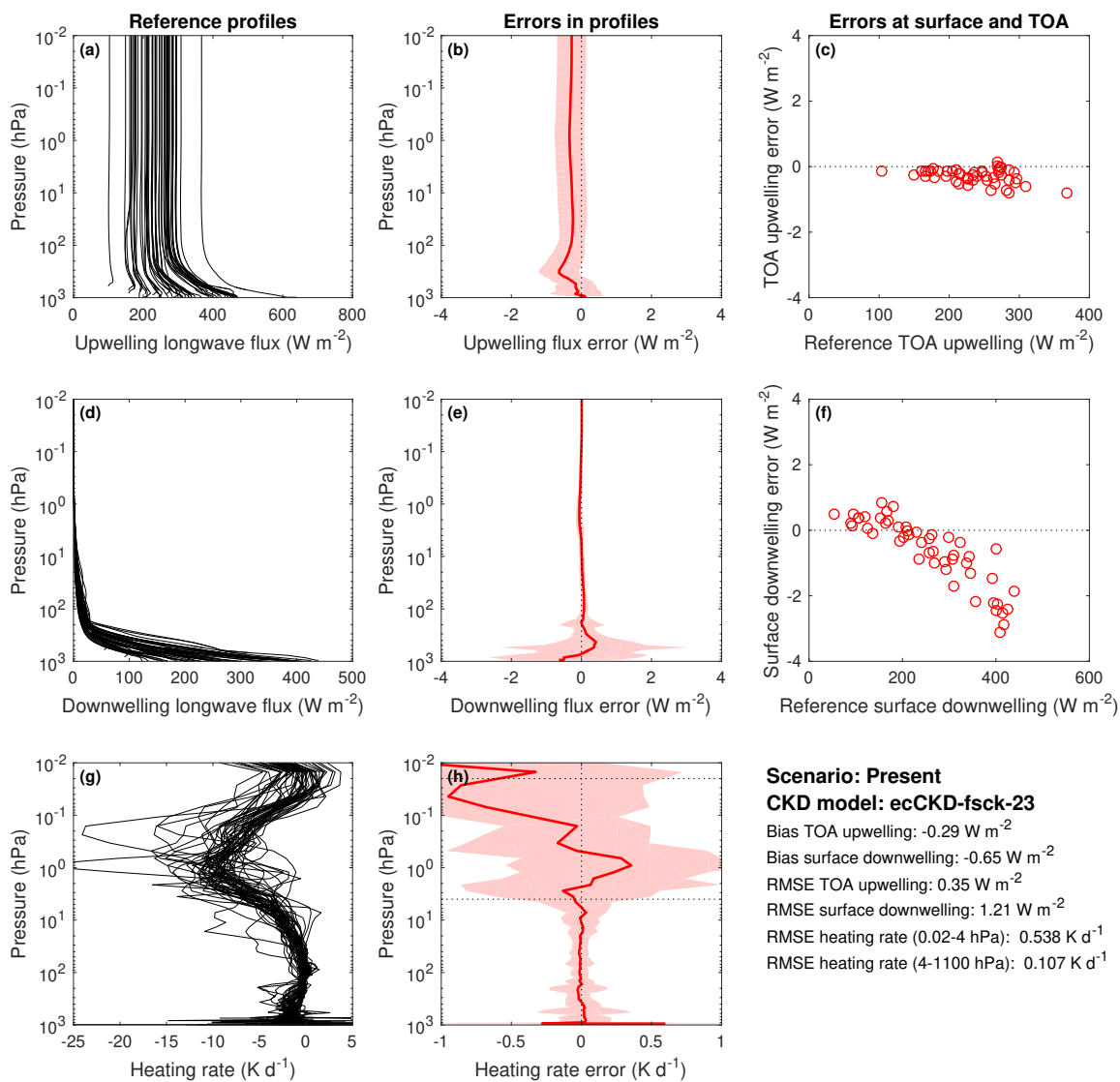


Illustration of the parts of the longwave spectrum that contribute to each k term of the limited-area-nwp-fsck-23 model.



Evaluation of the limited-area-nwp-fsck-23 CKD model for the “present-day” CKDMIP scenario. The left three panels show the irradiances and heating rates from the reference line-by-line calculations. The red lines in the middle three panels show the corresponding bias in these quantities from the CKD model. The shaded regions encompass 95% of the instantaneous errors. Panels c and f depict instantaneous errors in upwelling TOA and downwelling surface irradiances. Error metrics are provided in the lower right.

Model 5: ecCKD limited-area-nwp-fsck-35

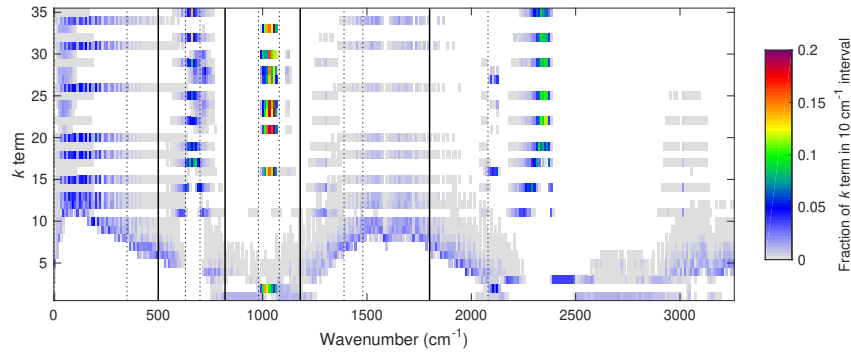
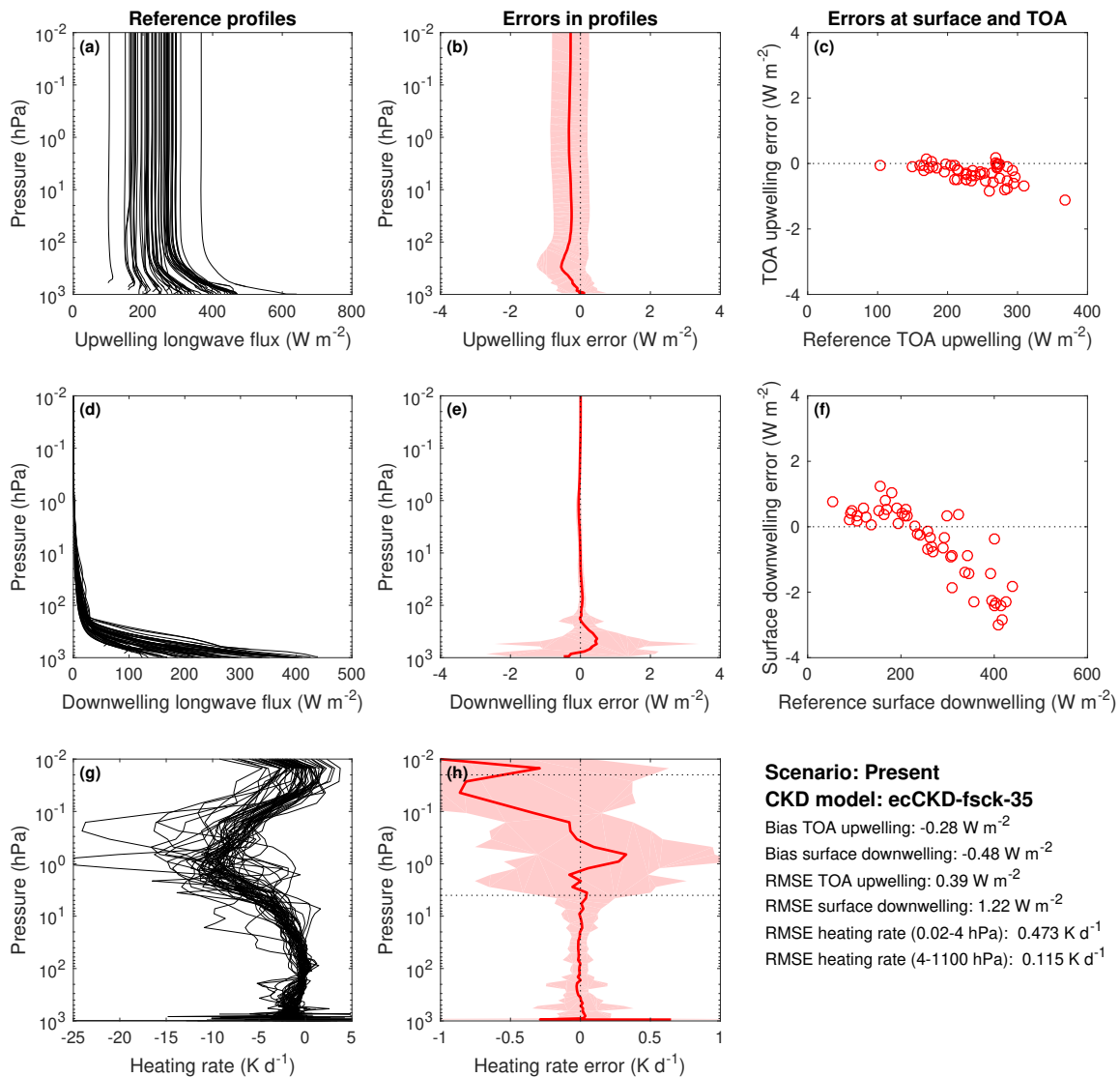


Illustration of the parts of the longwave spectrum that contribute to each k term of the limited-area-nwp-fsck-35 model.



Evaluation of the limited-area-nwp-fsck-35 CKD model for the “present-day” CKDMIP scenario. The left three panels show the irradiances and heating rates from the reference line-by-line calculations. The red lines in the middle three panels show the corresponding bias in these quantities from the CKD model. The shaded regions encompass 95% of the instantaneous errors. Panels c and f depict instantaneous errors in upwelling TOA and downwelling surface irradiances. Error metrics are provided in the lower right.

Model 6: ecCKD limited-area-nwp-fsck-55

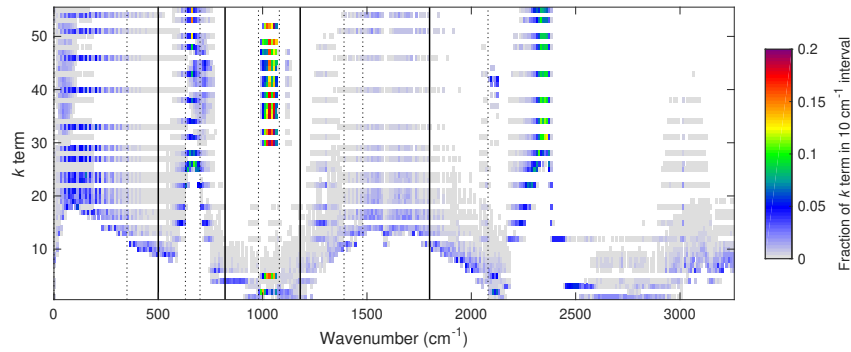
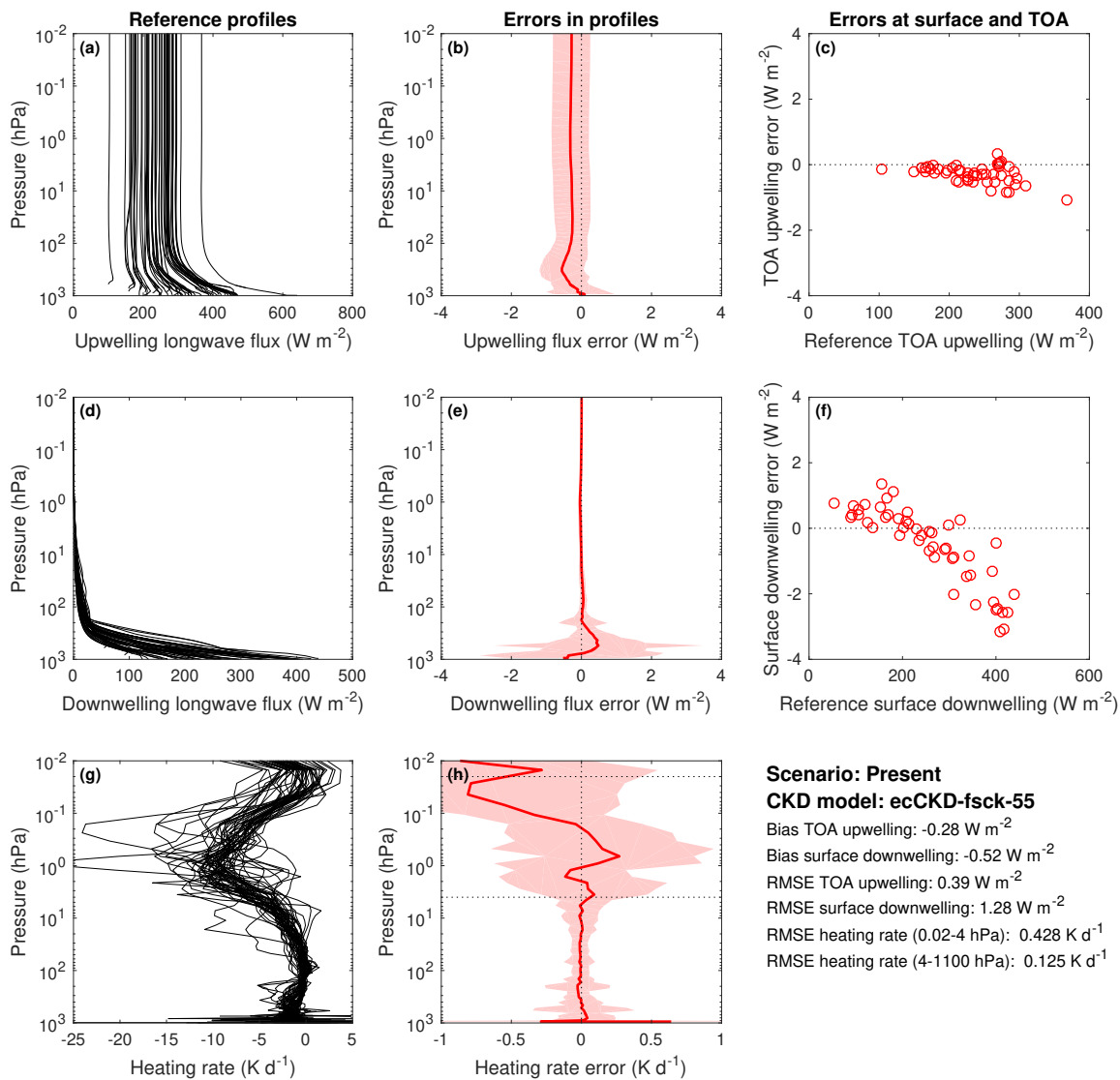


Illustration of the parts of the longwave spectrum that contribute to each k term of the limited-area-nwp-fsck-55 model.



Evaluation of the limited-area-nwp-fsck-55 CKD model for the “present-day” CKDMIP scenario. The left three panels show the irradiances and heating rates from the reference line-by-line calculations. The red lines in the middle three panels show the corresponding bias in these quantities from the CKD model. The shaded regions encompass 95% of the instantaneous errors. Panels c and f depict instantaneous errors in upwelling TOA and downwelling surface irradiances. Error metrics are provided in the lower right.

Model 7: ecCKD limited-area-nwp-wide-10

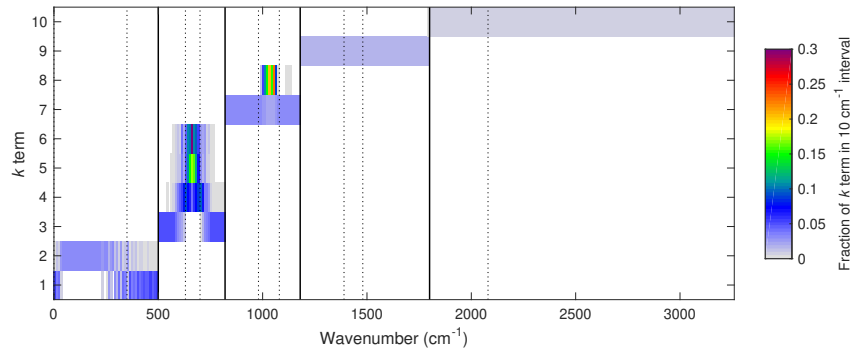
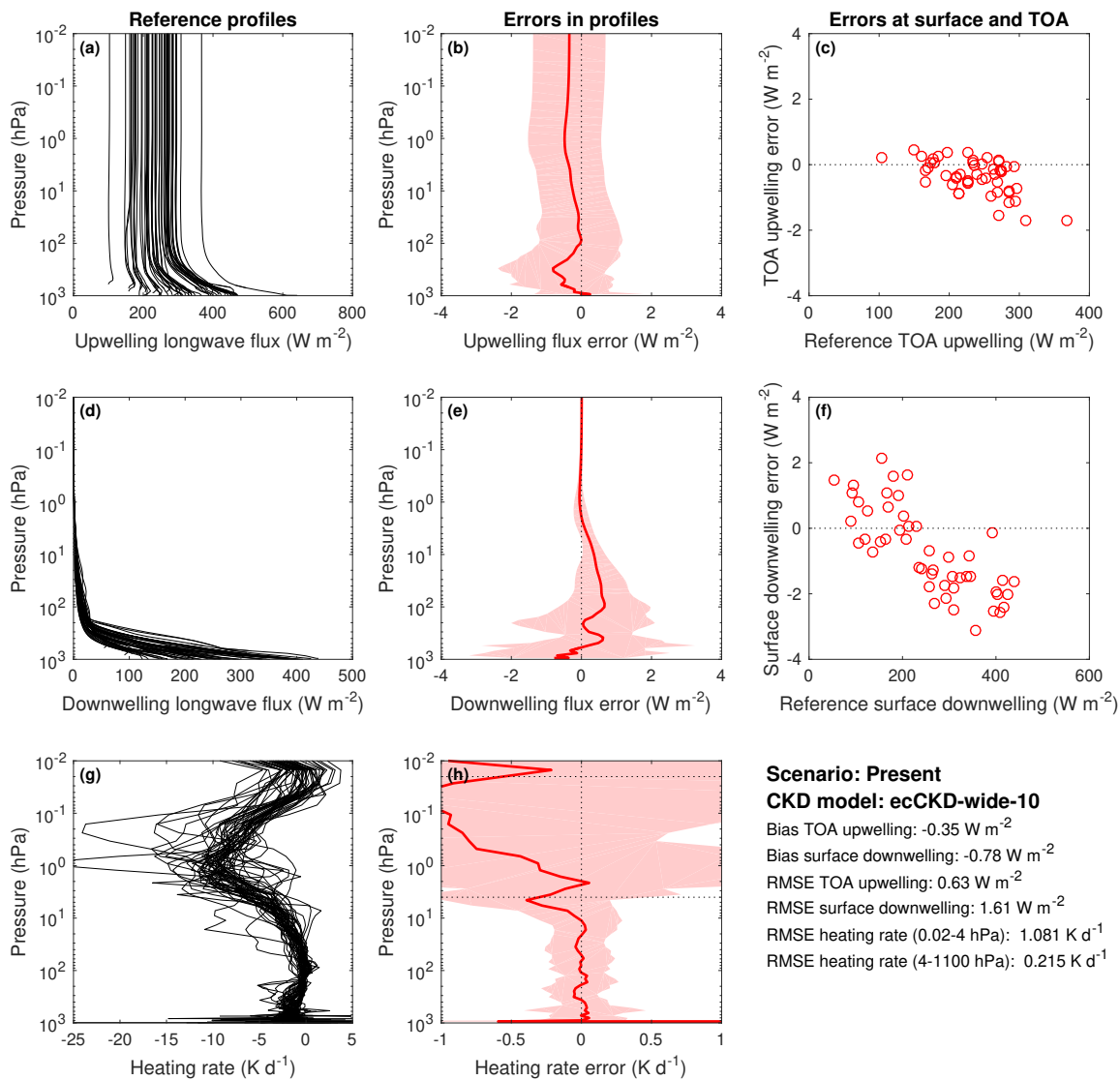
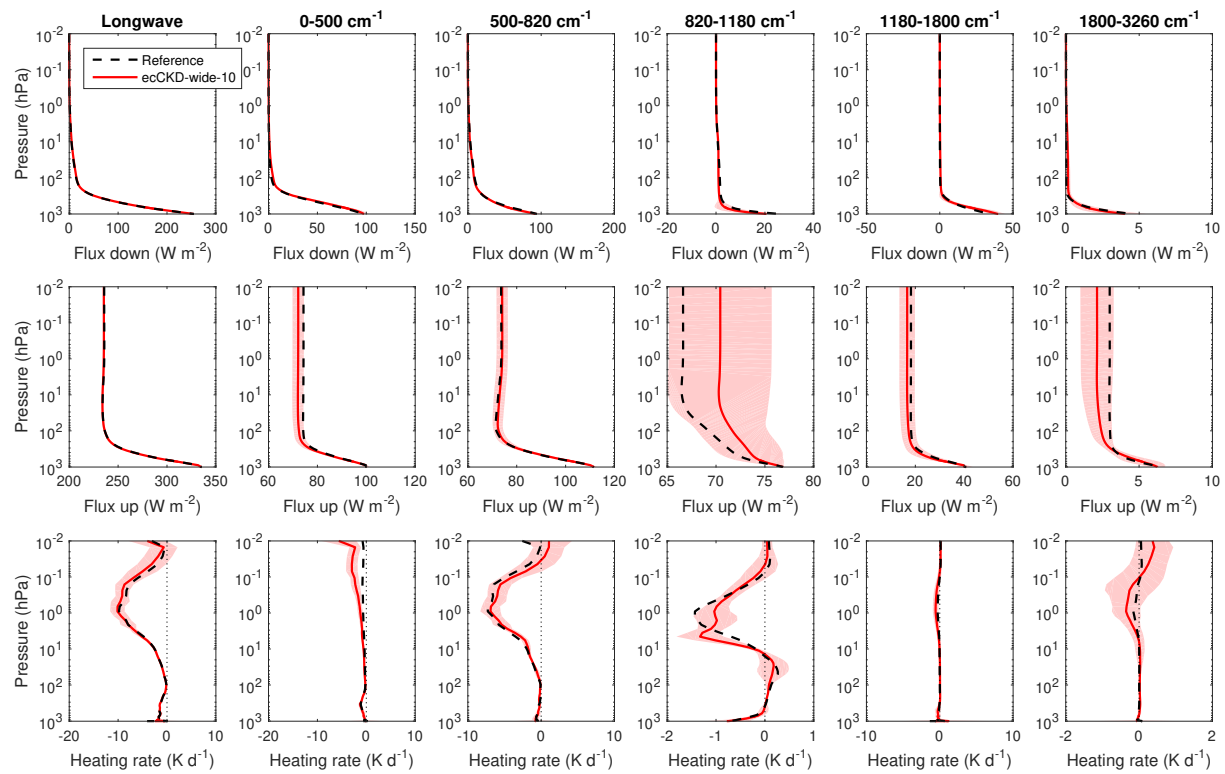


Illustration of the parts of the longwave spectrum that contribute to each k term of the limited-area-nwp-wide-10 model.



Evaluation of the limited-area-nwp-wide-10 CKD model for the “present-day” CKDMIP scenario. The left three panels show the irradiances and heating rates from the reference line-by-line calculations. The red lines in the middle three panels show the corresponding bias in these quantities from the CKD model. The shaded regions encompass 95% of the instantaneous errors. Panels c and f depict instantaneous errors in upwelling TOA and downwelling surface irradiances. Error metrics are provided in the lower right.



Evaluation of irradiances and heating rates for the broadband (leftmost column of panels) and the 5 wide long-wave bands (other panels) of the limited-area-nwp-wide-10 CKD model. The black dashed and red solid lines correspond to the average of the 50 profiles for the “present-day” scenario, while the shaded regions encompass 95% of the error.

Model 8: ecCKD limited-area-nwp-wide-15

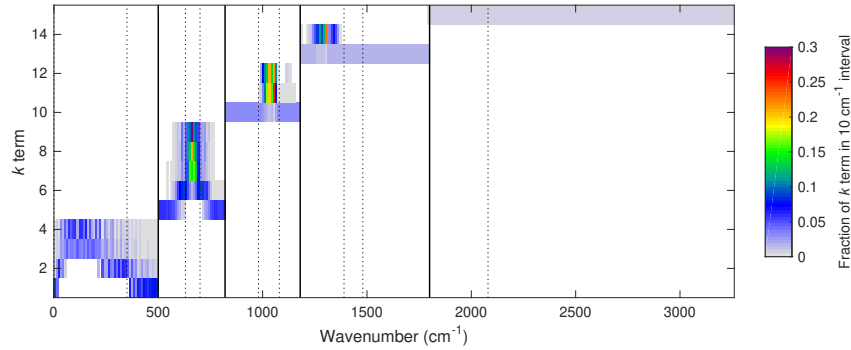
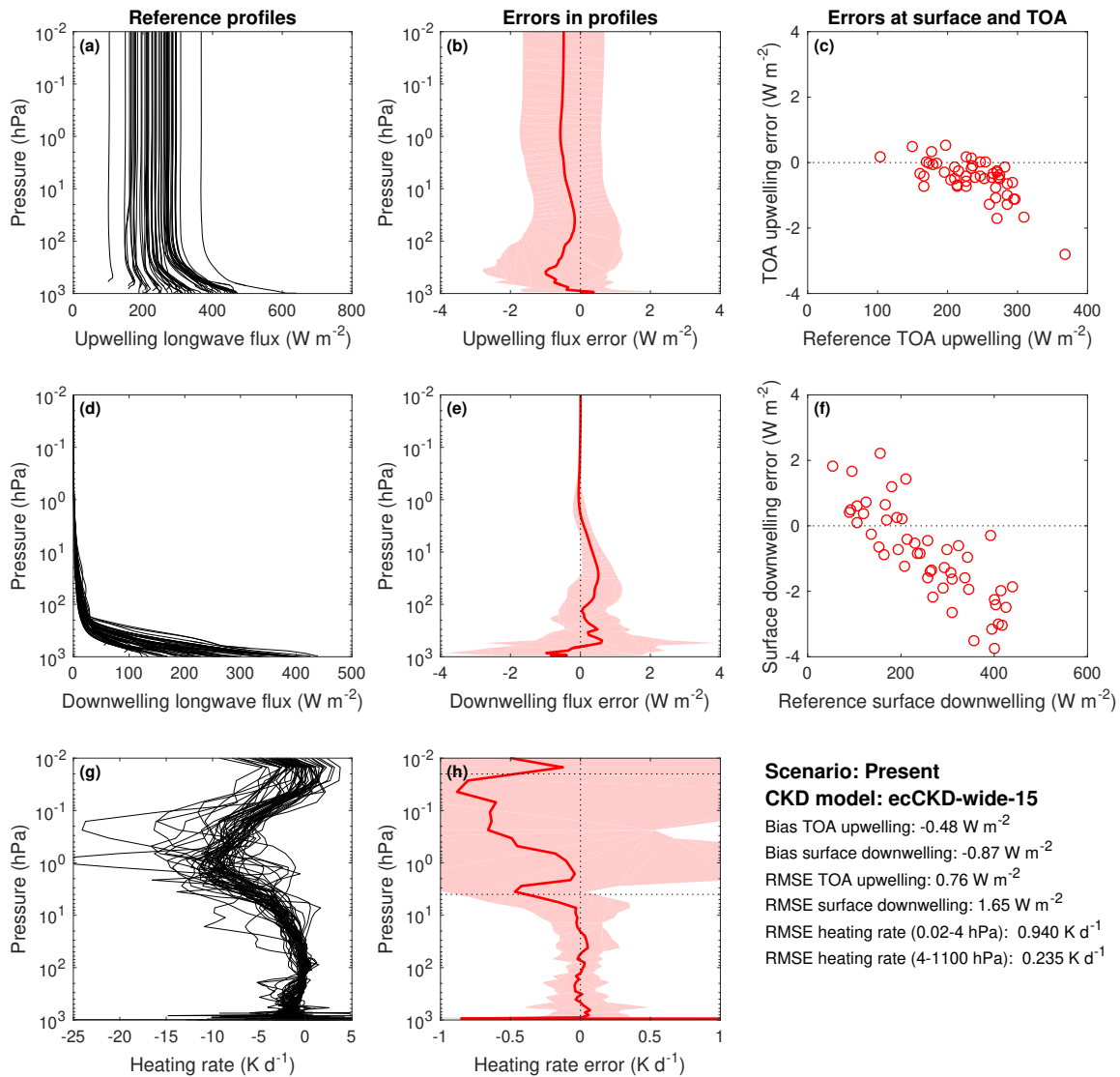
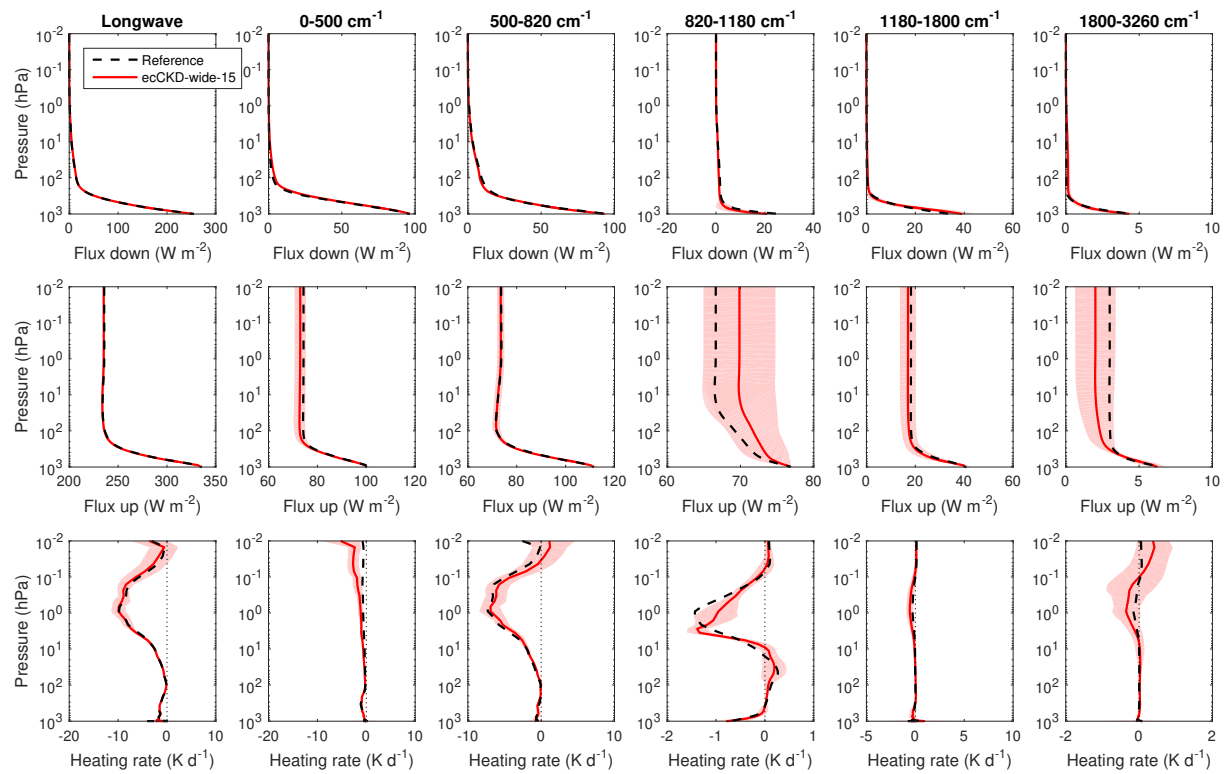


Illustration of the parts of the longwave spectrum that contribute to each k term of the limited-area-nwp-wide-15 model.



Evaluation of the limited-area-nwp-wide-15 CKD model for the “present-day” CKDMIP scenario. The left three panels show the irradiances and heating rates from the reference line-by-line calculations. The red lines in the middle three panels show the corresponding bias in these quantities from the CKD model. The shaded regions encompass 95% of the instantaneous errors. Panels c and f depict instantaneous errors in upwelling TOA and downwelling surface irradiances. Error metrics are provided in the lower right.



Evaluation of irradiances and heating rates for the broadband (leftmost column of panels) and the 5 wide long-wave bands (other panels) of the limited-area-nwp-wide-15 CKD model. The black dashed and red solid lines correspond to the average of the 50 profiles for the “present-day” scenario, while the shaded regions encompass 95% of the error.

Model 9: ecCKD limited-area-nwp-wide-23

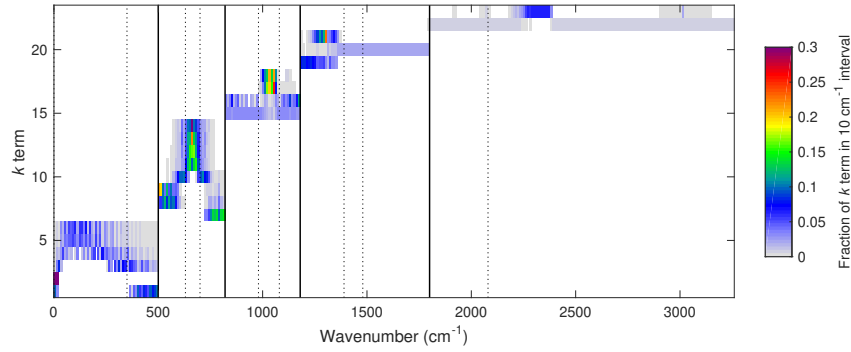
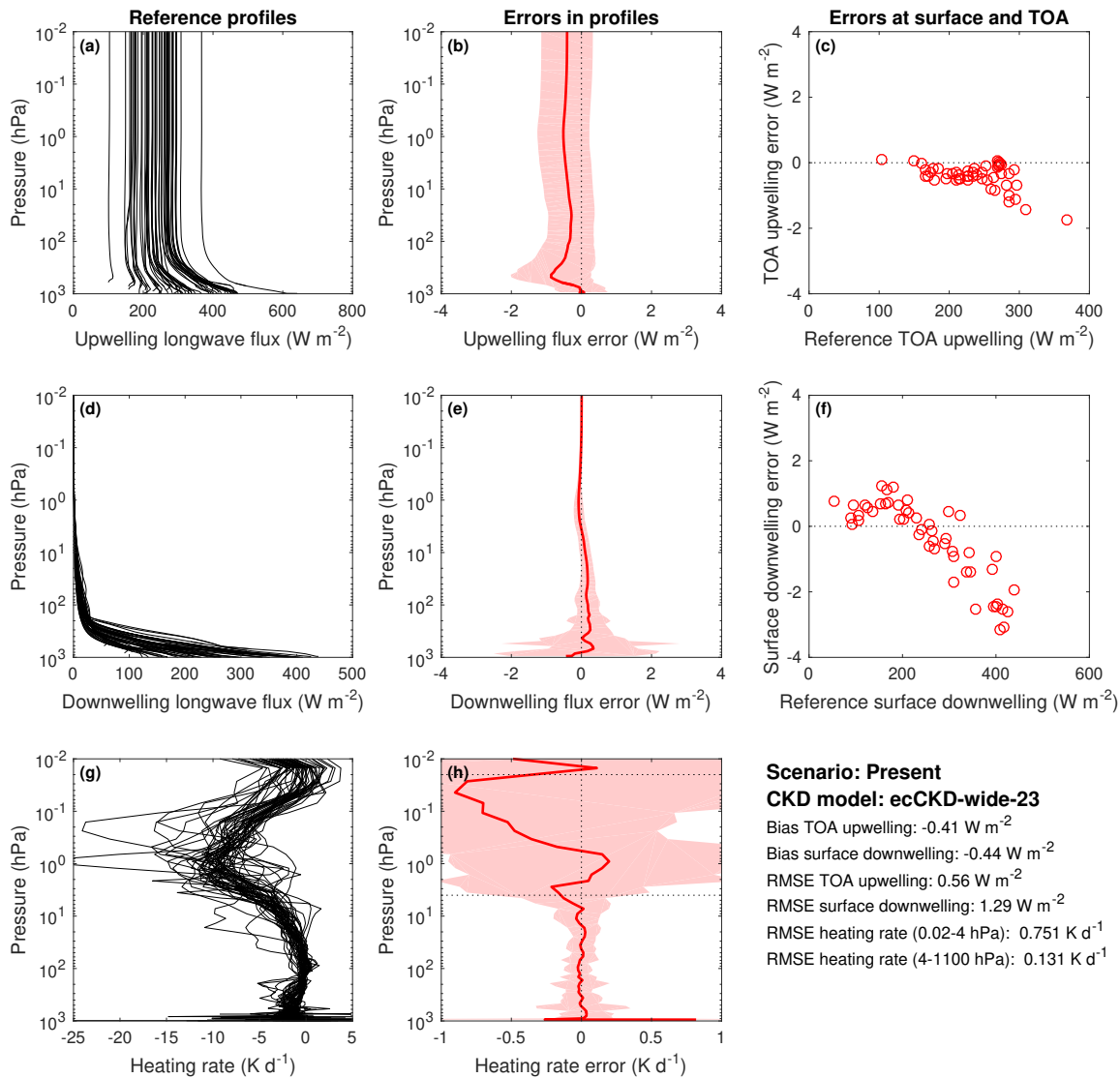
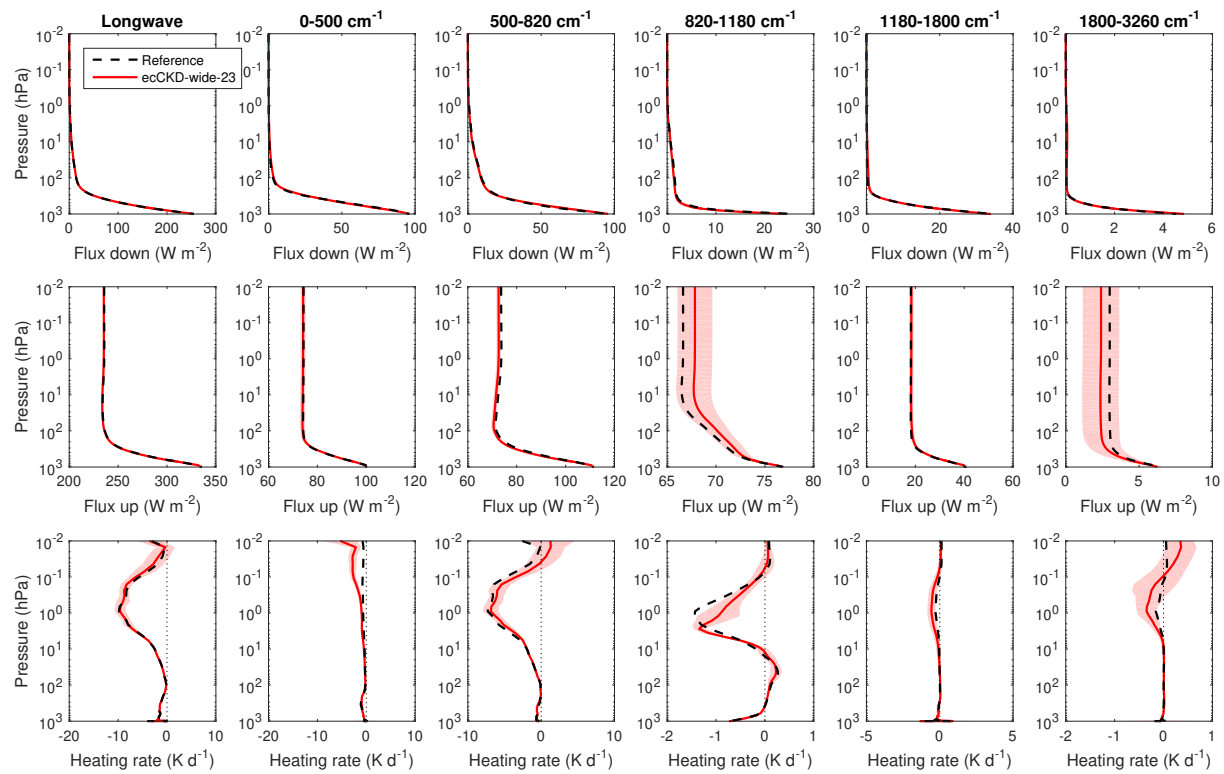


Illustration of the parts of the longwave spectrum that contribute to each k term of the limited-area-nwp-wide-23 model.



Evaluation of the limited-area-nwp-wide-23 CKD model for the “present-day” CKDMIP scenario. The left three panels show the irradiances and heating rates from the reference line-by-line calculations. The red lines in the middle three panels show the corresponding bias in these quantities from the CKD model. The shaded regions encompass 95% of the instantaneous errors. Panels c and f depict instantaneous errors in upwelling TOA and downwelling surface irradiances. Error metrics are provided in the lower right.



Evaluation of irradiances and heating rates for the broadband (leftmost column of panels) and the 5 wide long-wave bands (other panels) of the limited-area-nwp-wide-23 CKD model. The black dashed and red solid lines correspond to the average of the 50 profiles for the “present-day” scenario, while the shaded regions encompass 95% of the error.

Model 10: ecCKD limited-area-nwp-wide-31

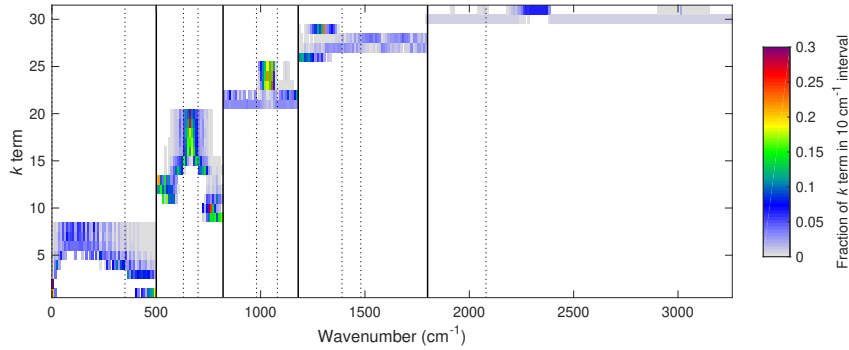
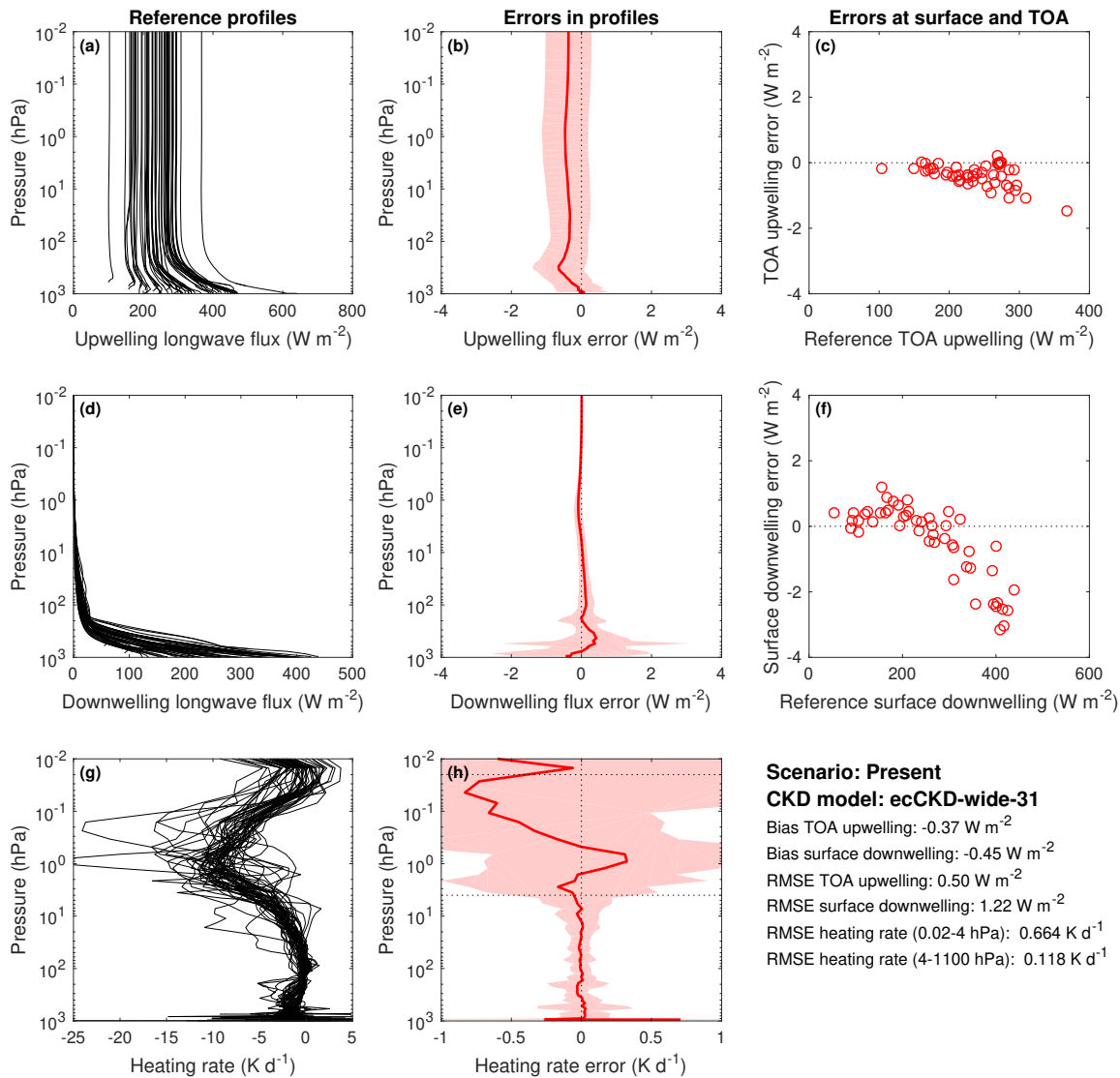
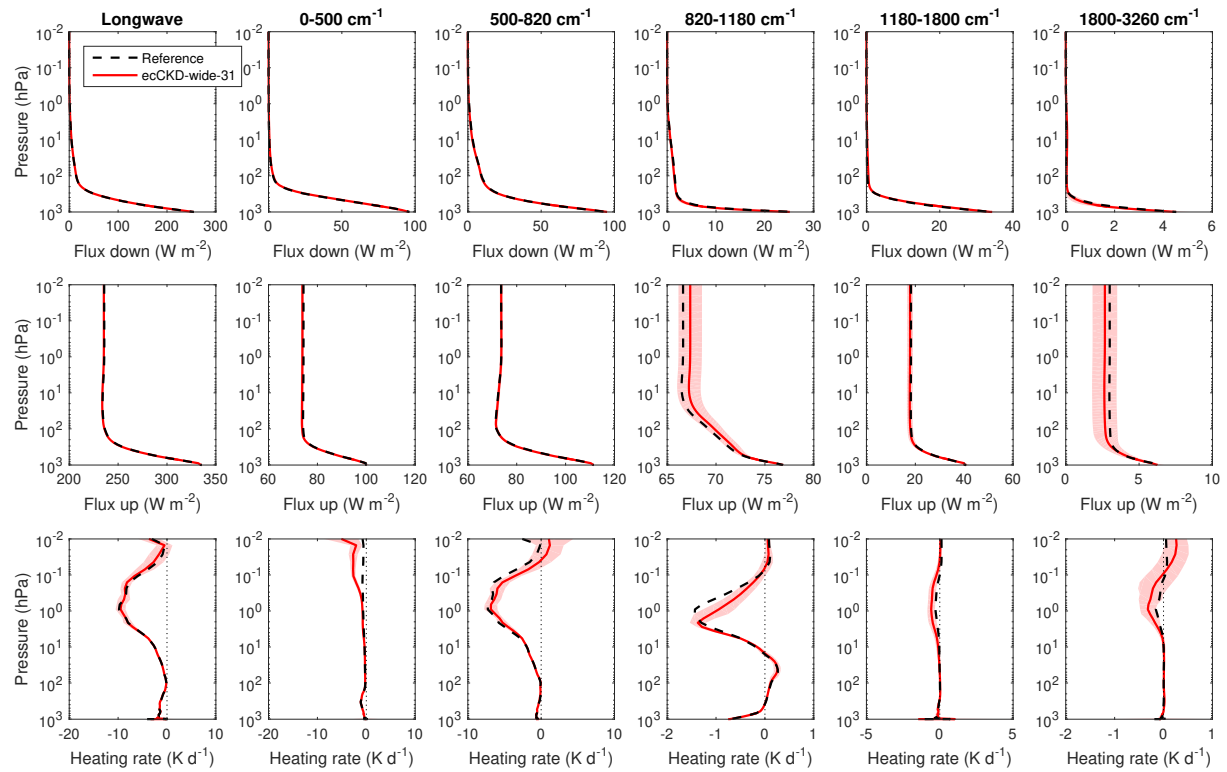


Illustration of the parts of the longwave spectrum that contribute to each k term of the limited-area-nwp-wide-31 model.



Evaluation of the limited-area-nwp-wide-31 CKD model for the “present-day” CKDMIP scenario. The left three panels show the irradiances and heating rates from the reference line-by-line calculations. The red lines in the middle three panels show the corresponding bias in these quantities from the CKD model. The shaded regions encompass 95% of the instantaneous errors. Panels c and f depict instantaneous errors in upwelling TOA and downwelling surface irradiances. Error metrics are provided in the lower right.



Evaluation of irradiances and heating rates for the broadband (leftmost column of panels) and the 5 wide long-wave bands (other panels) of the limited-area-nwp-wide-31 CKD model. The black dashed and red solid lines correspond to the average of the 50 profiles for the “present-day” scenario, while the shaded regions encompass 95% of the error.

Model 11: ecCKD limited-area-nwp-wide-42

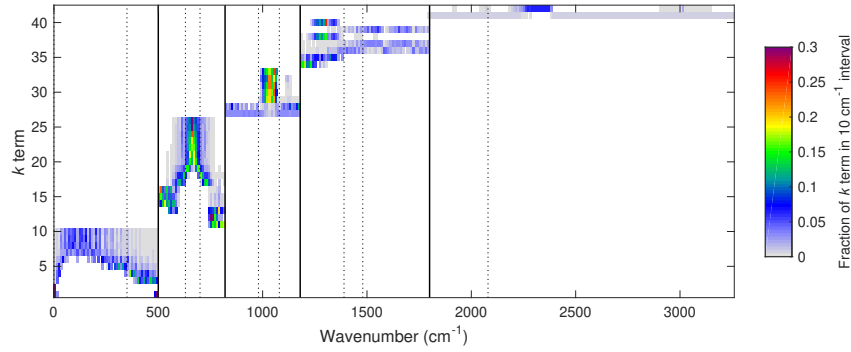
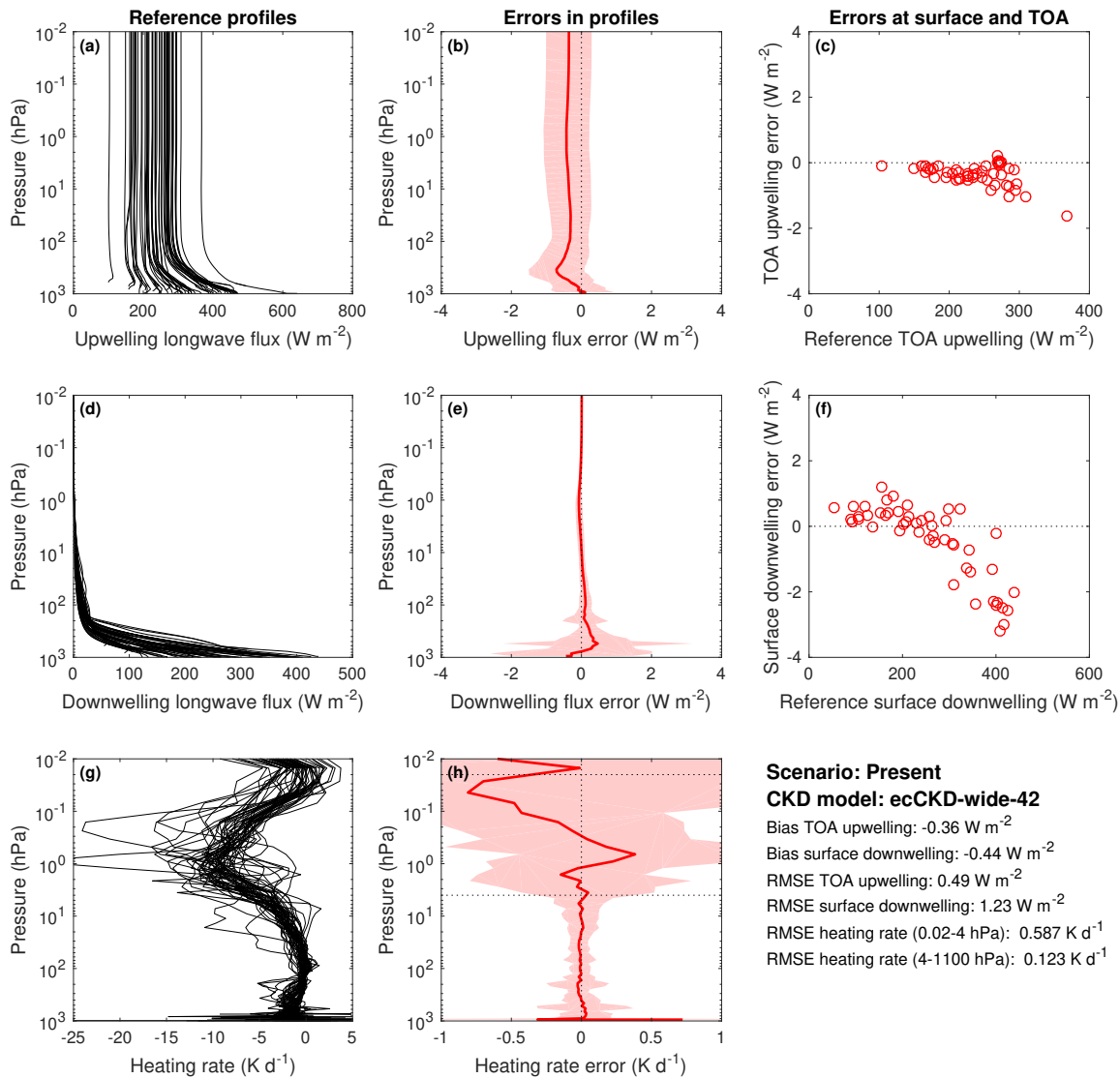
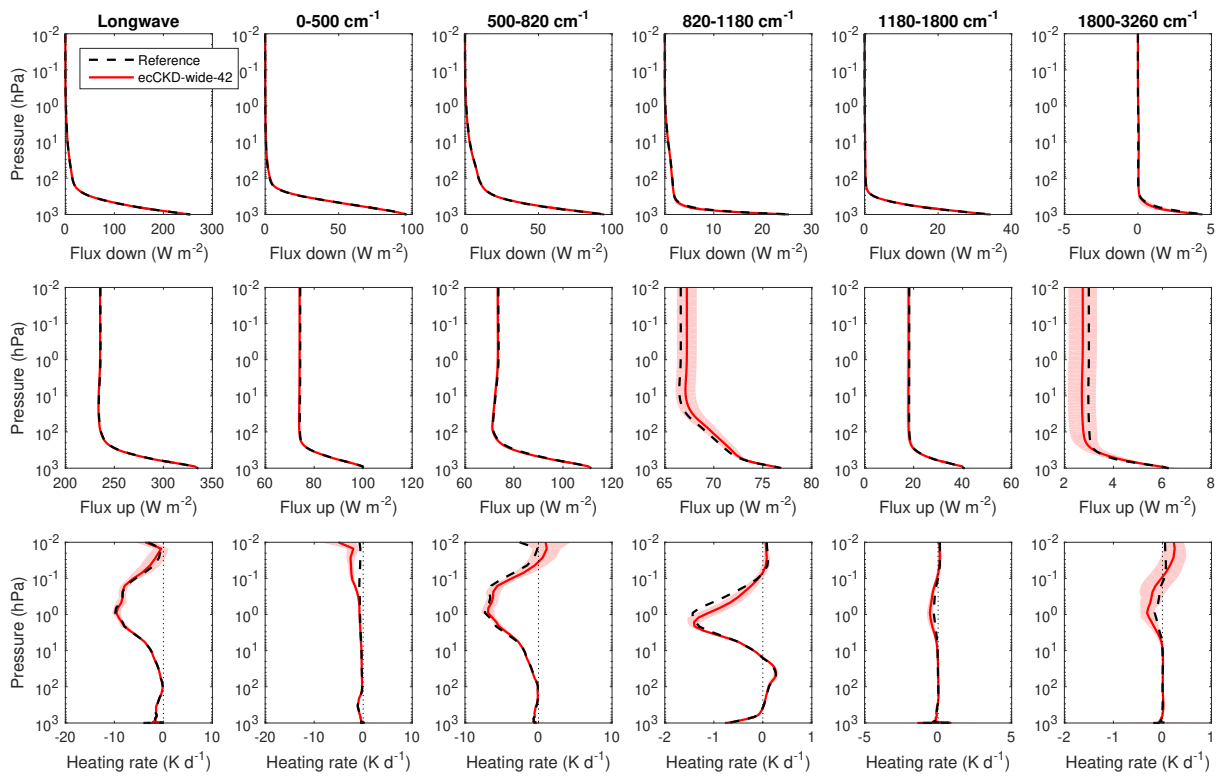


Illustration of the parts of the longwave spectrum that contribute to each k term of the limited-area-nwp-wide-42 model.



Evaluation of the limited-area-nwp-wide-42 CKD model for the “present-day” CKDMIP scenario. The left three panels show the irradiances and heating rates from the reference line-by-line calculations. The red lines in the middle three panels show the corresponding bias in these quantities from the CKD model. The shaded regions encompass 95% of the instantaneous errors. Panels c and f depict instantaneous errors in upwelling TOA and downwelling surface irradiances. Error metrics are provided in the lower right.



Evaluation of irradiances and heating rates for the broadband (leftmost column of panels) and the 5 wide long-wave bands (other panels) of the limited-area-nwp-wide-42 CKD model. The black dashed and red solid lines correspond to the average of the 50 profiles for the “present-day” scenario, while the shaded regions encompass 95% of the error.

Model 12: ecCKD limited-area-nwp-wide-61

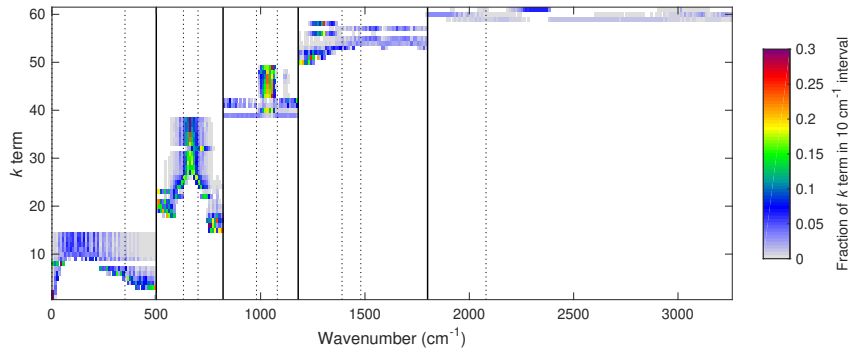
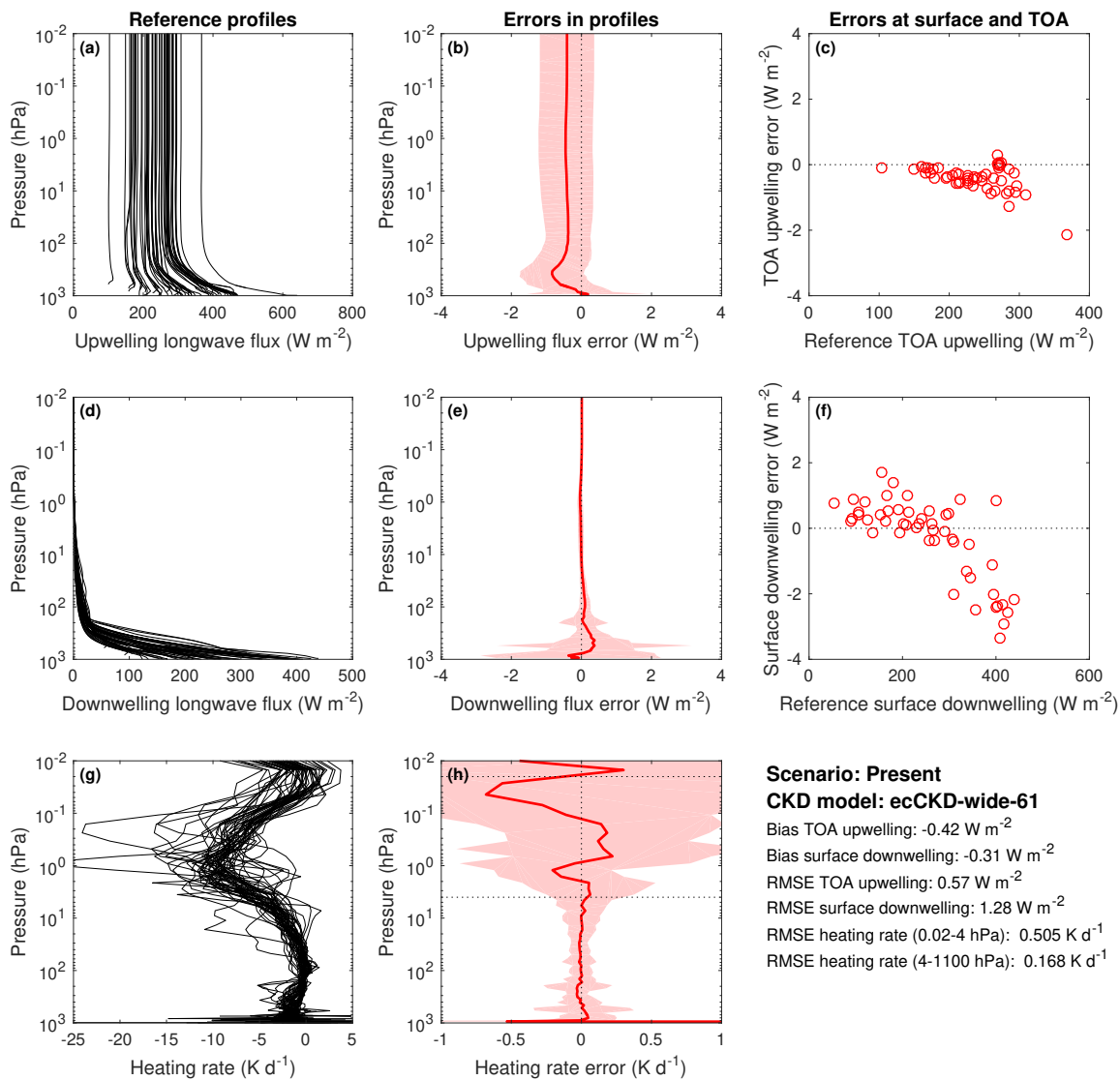
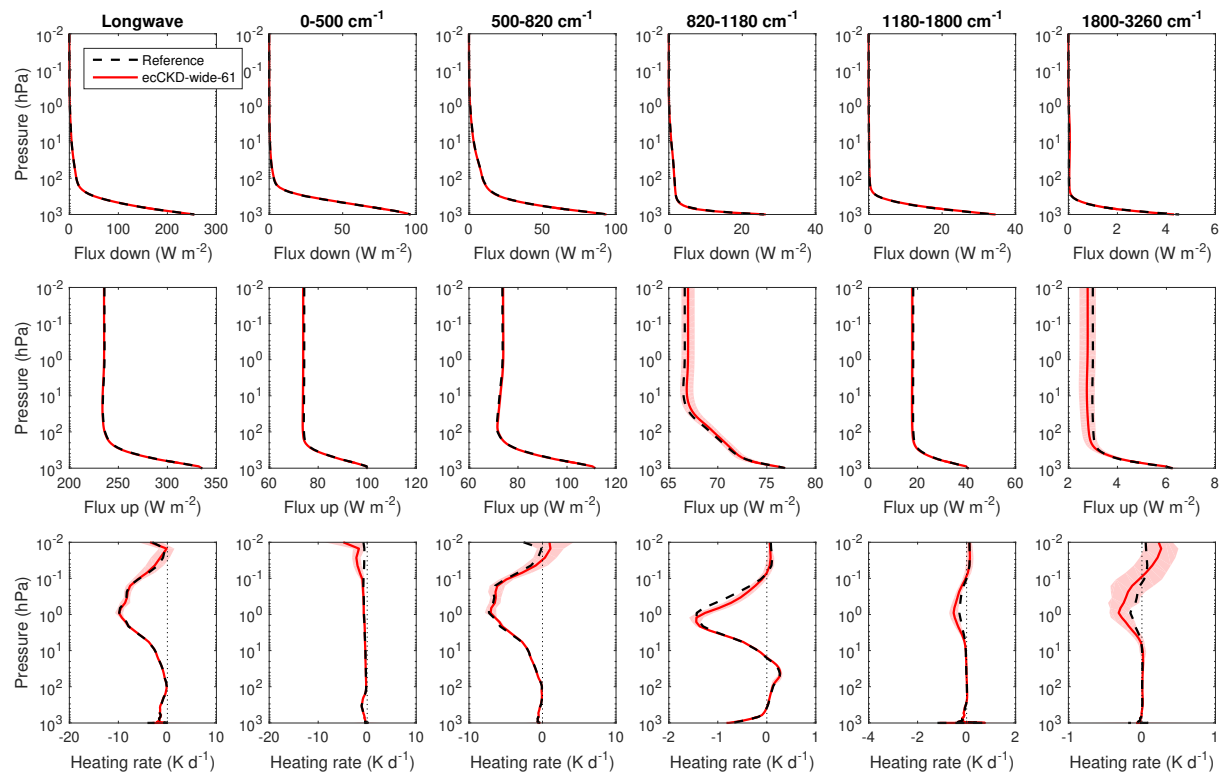


Illustration of the parts of the longwave spectrum that contribute to each k term of the limited-area-nwp-wide-61 model.



Evaluation of the limited-area-nwp-wide-61 CKD model for the “present-day” CKDMIP scenario. The left three panels show the irradiances and heating rates from the reference line-by-line calculations. The red lines in the middle three panels show the corresponding bias in these quantities from the CKD model. The shaded regions encompass 95% of the instantaneous errors. Panels c and f depict instantaneous errors in upwelling TOA and downwelling surface irradiances. Error metrics are provided in the lower right.



Evaluation of irradiances and heating rates for the broadband (leftmost column of panels) and the 5 wide long-wave bands (other panels) of the limited-area-nwp-wide-61 CKD model. The black dashed and red solid lines correspond to the average of the 50 profiles for the “present-day” scenario, while the shaded regions encompass 95% of the error.

Model 13: ecCKD limited-area-nwp-narrow-17

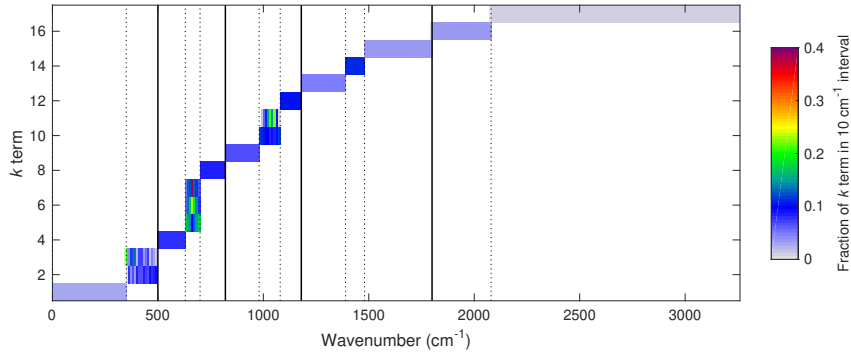
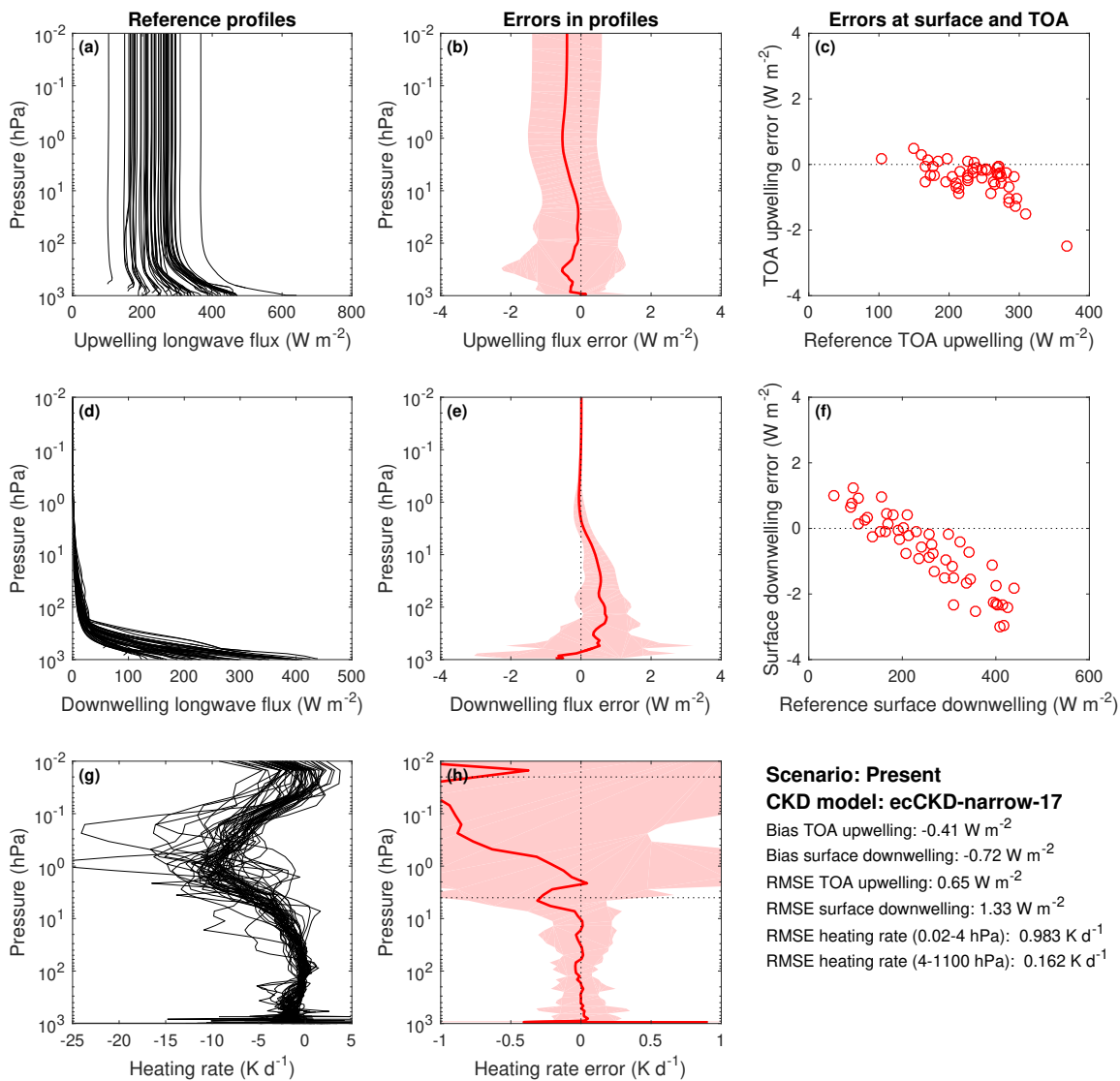
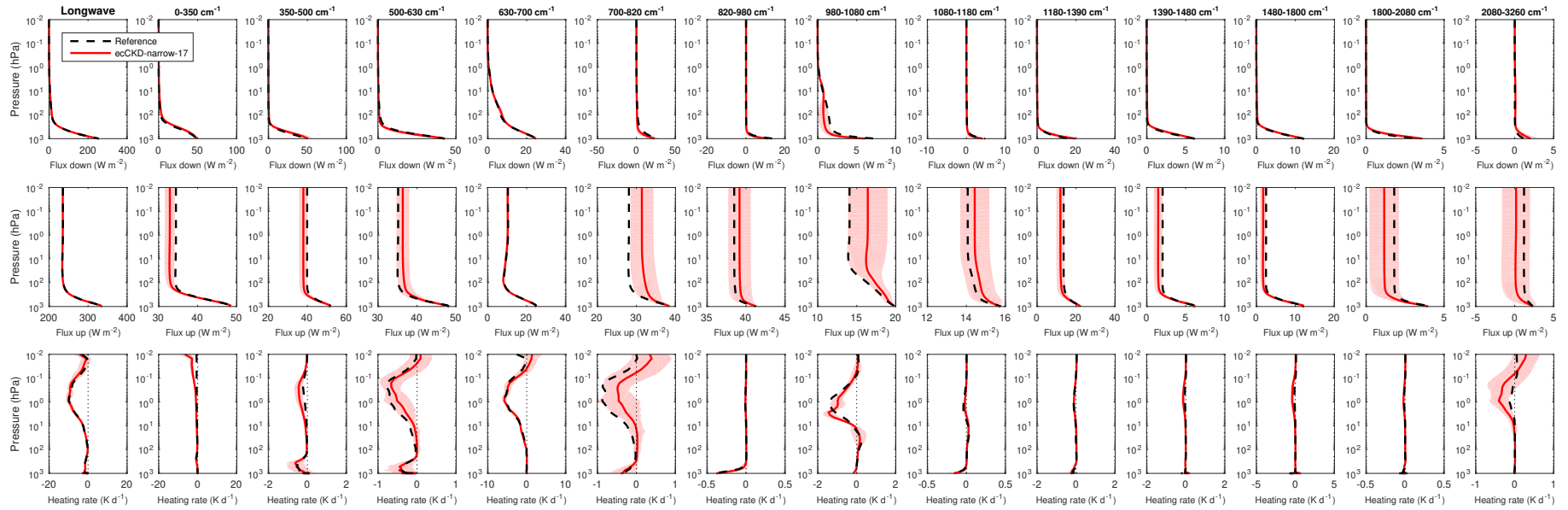


Illustration of the parts of the longwave spectrum that contribute to each k term of the limited-area-nwp-narrow-17 model.



Evaluation of the limited-area-nwp-narrow-17 CKD model for the “present-day” CKDMIP scenario. The left three panels show the irradiances and heating rates from the reference line-by-line calculations. The red lines in the middle three panels show the corresponding bias in these quantities from the CKD model. The shaded regions encompass 95% of the instantaneous errors. Panels c and f depict instantaneous errors in upwelling TOA and downwelling surface irradiances. Error metrics are provided in the lower right.



Evaluation of irradiances and heating rates for the broadband (leftmost column of panels) and the 13 narrow longwave bands (other panels) of the limited-area-nwp-narrow-17 CKD model. The black dashed and red solid lines correspond to the average of the 50 profiles for the “present-day” scenario, while the shaded regions encompass 95% of the error.

Model 14: ecCKD limited-area-nwp-narrow-25

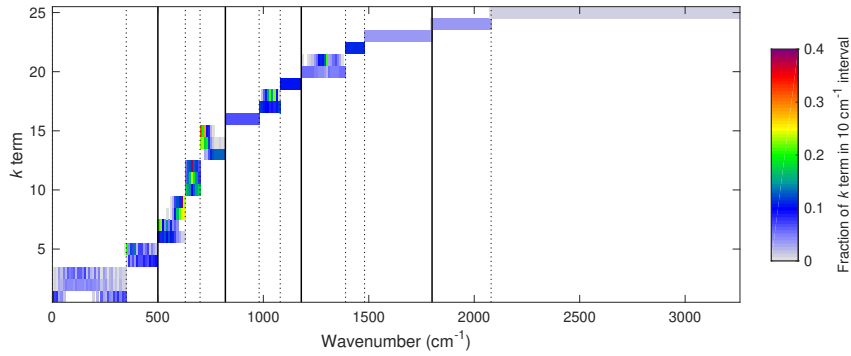
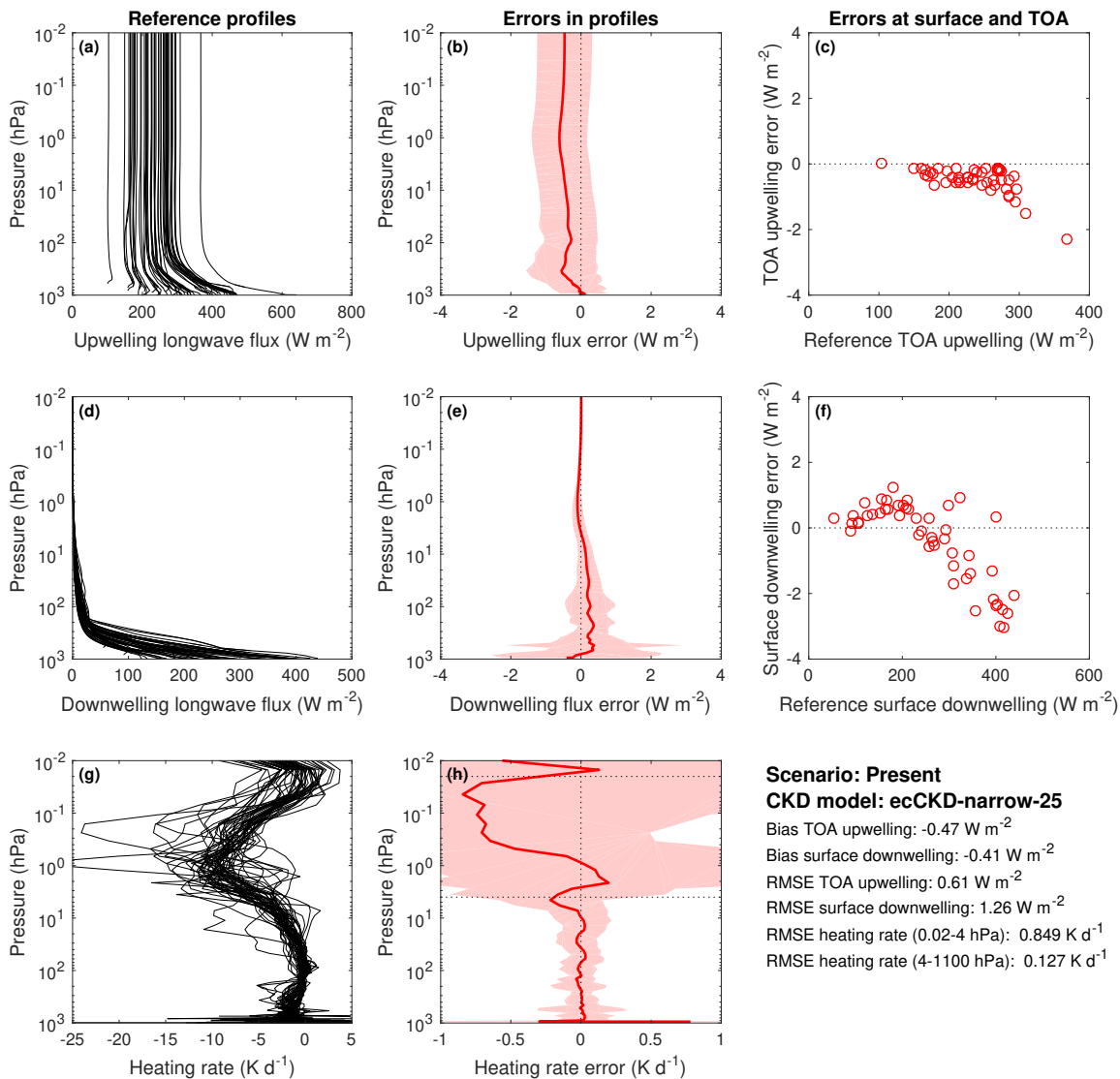
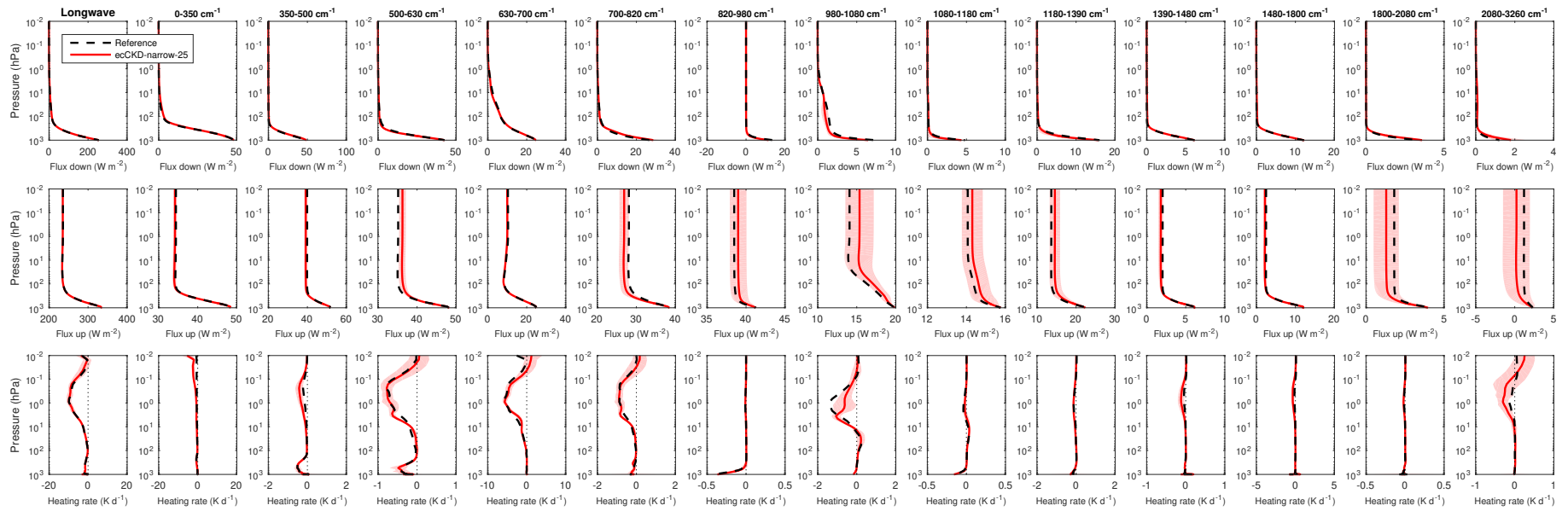


Illustration of the parts of the longwave spectrum that contribute to each k term of the limited-area-nwp-narrow-25 model.



Evaluation of the limited-area-nwp-narrow-25 CKD model for the “present-day” CKDMIP scenario. The left three panels show the irradiances and heating rates from the reference line-by-line calculations. The red lines in the middle three panels show the corresponding bias in these quantities from the CKD model. The shaded regions encompass 95% of the instantaneous errors. Panels c and f depict instantaneous errors in upwelling TOA and downwelling surface irradiances. Error metrics are provided in the lower right.



Evaluation of irradiances and heating rates for the broadband (leftmost column of panels) and the 13 narrow longwave bands (other panels) of the limited-area-nwp-narrow-25 CKD model. The black dashed and red solid lines correspond to the average of the 50 profiles for the “present-day” scenario, while the shaded regions encompass 95% of the error.

Model 15: ecCKD limited-area-nwp-narrow-28

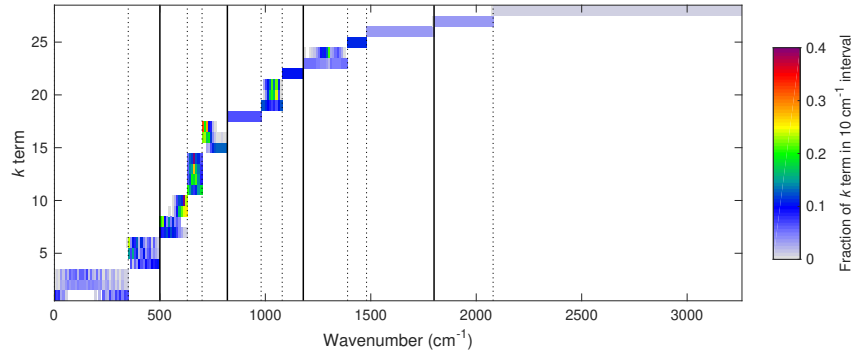
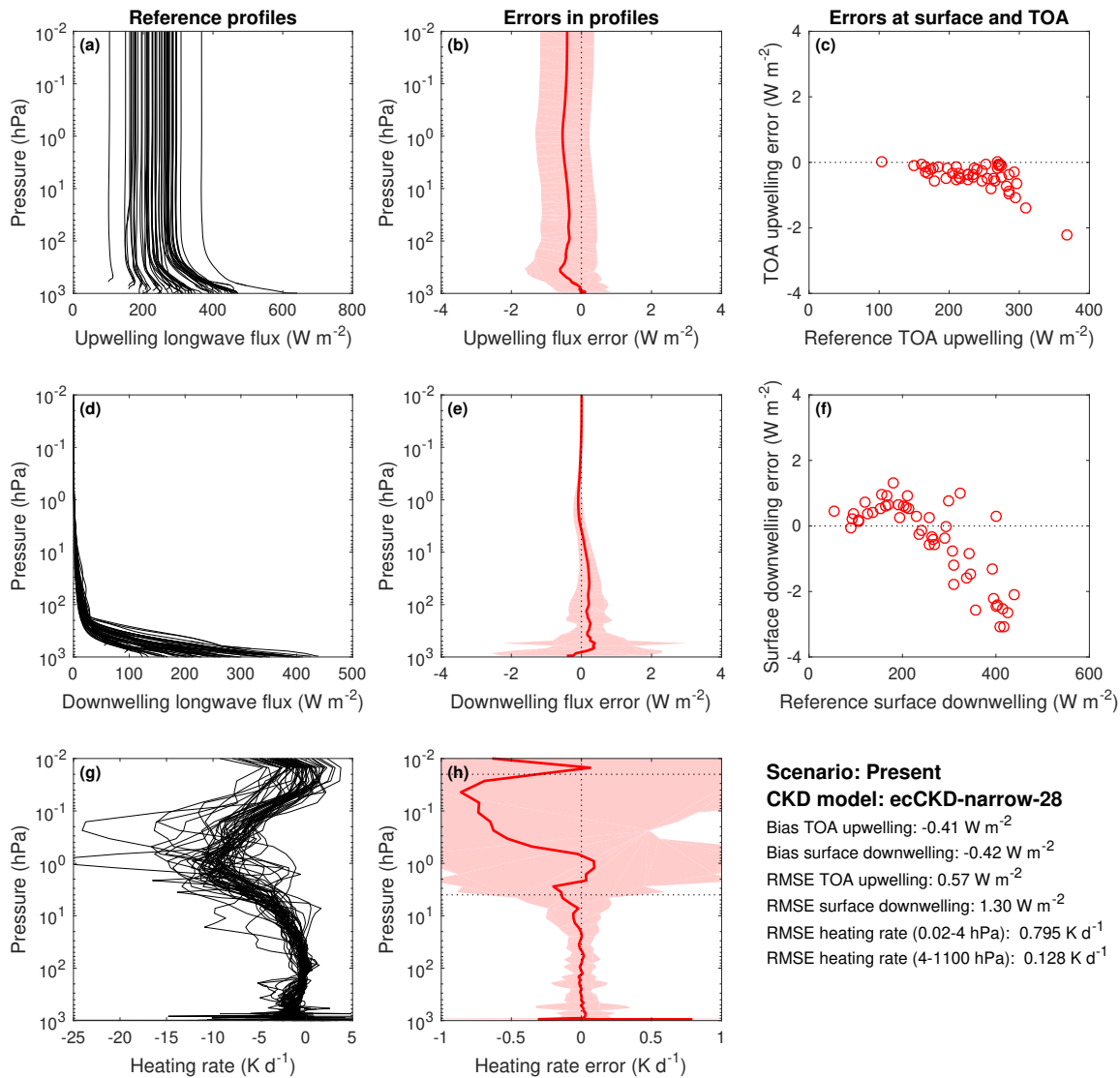
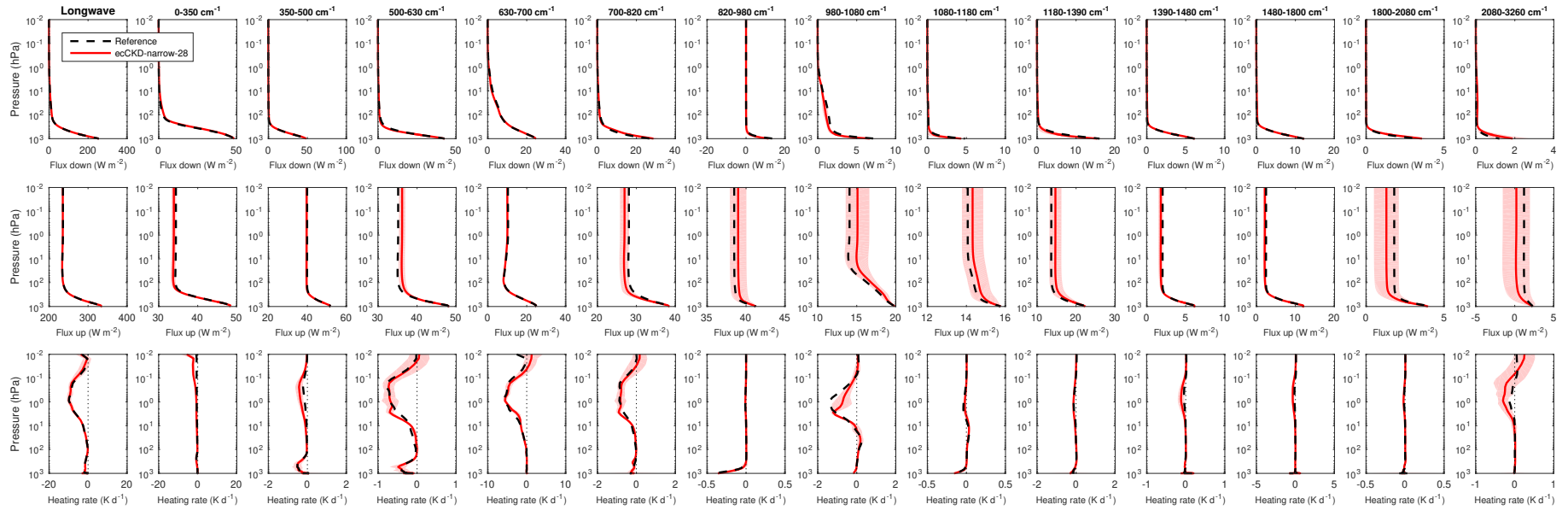


Illustration of the parts of the longwave spectrum that contribute to each k term of the limited-area-nwp-narrow-28 model.



Evaluation of the limited-area-nwp-narrow-28 CKD model for the “present-day” CKDMIP scenario. The left three panels show the irradiances and heating rates from the reference line-by-line calculations. The red lines in the middle three panels show the corresponding bias in these quantities from the CKD model. The shaded regions encompass 95% of the instantaneous errors. Panels c and f depict instantaneous errors in upwelling TOA and downwelling surface irradiances. Error metrics are provided in the lower right.



Evaluation of irradiances and heating rates for the broadband (leftmost column of panels) and the 13 narrow longwave bands (other panels) of the limited-area-nwp-narrow-28 CKD model. The black dashed and red solid lines correspond to the average of the 50 profiles for the “present-day” scenario, while the shaded regions encompass 95% of the error.

Model 16: ecCKD limited-area-nwp-narrow-39

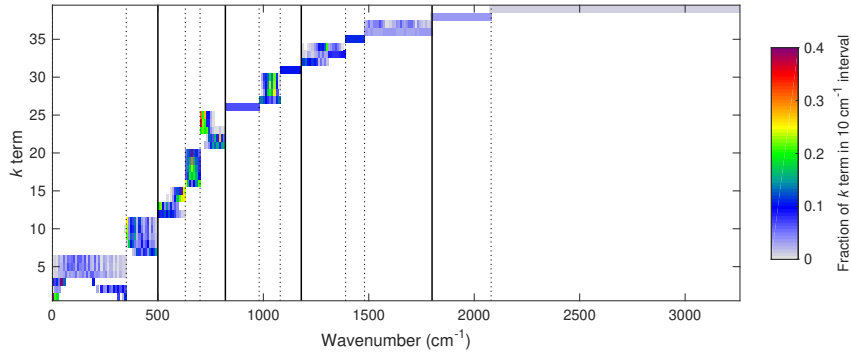
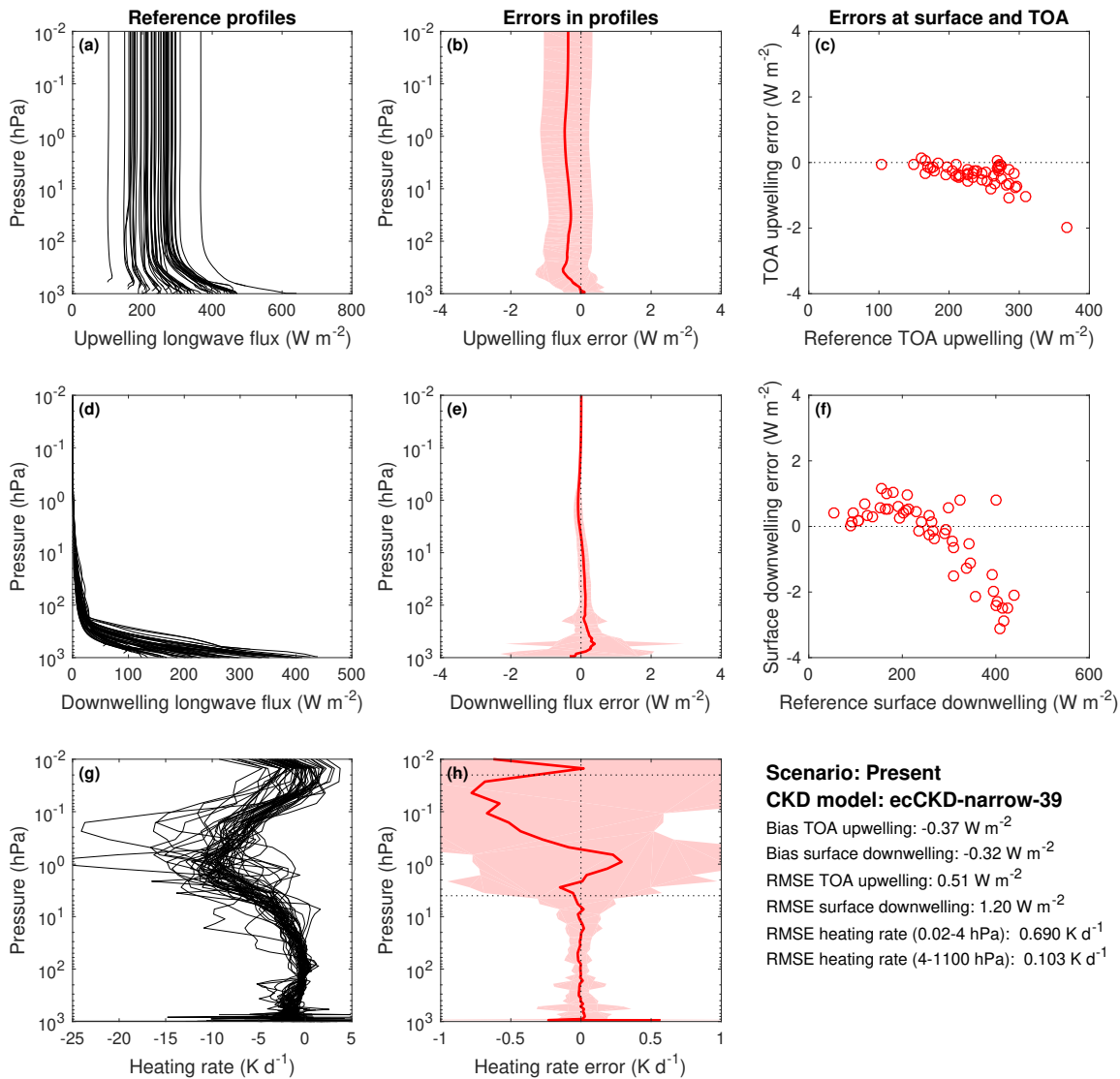
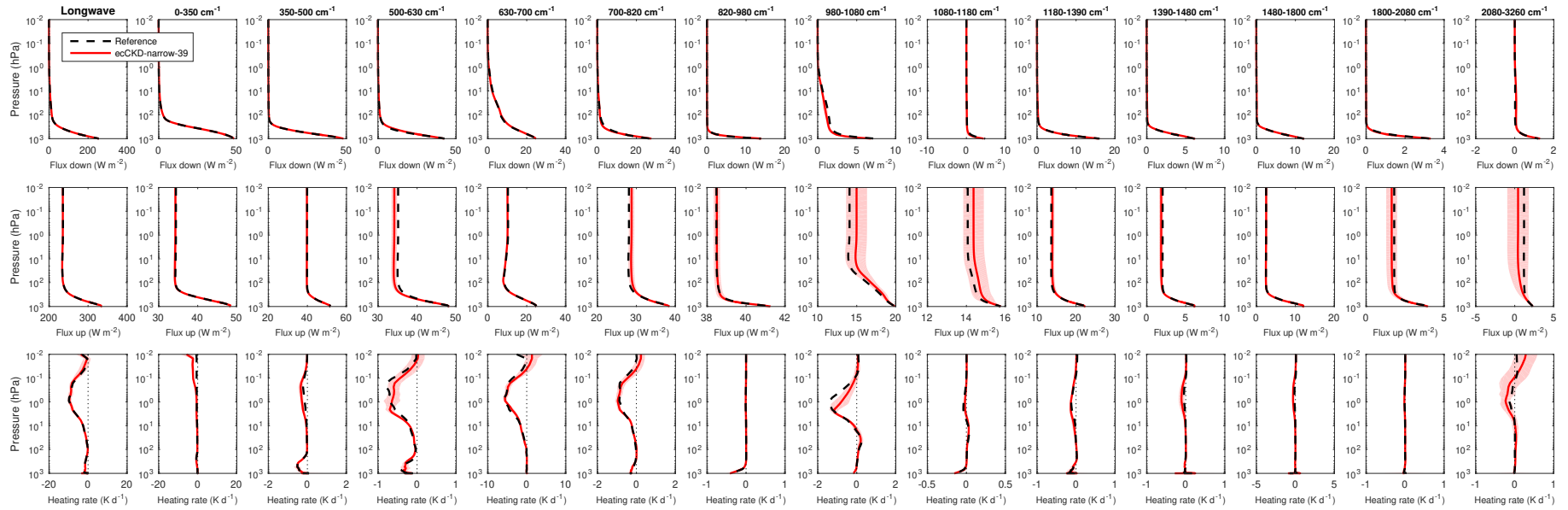


Illustration of the parts of the longwave spectrum that contribute to each k term of the limited-area-nwp-narrow-39 model.



Evaluation of the limited-area-nwp-narrow-39 CKD model for the “present-day” CKDMIP scenario. The left three panels show the irradiances and heating rates from the reference line-by-line calculations. The red lines in the middle three panels show the corresponding bias in these quantities from the CKD model. The shaded regions encompass 95% of the instantaneous errors. Panels c and f depict instantaneous errors in upwelling TOA and downwelling surface irradiances. Error metrics are provided in the lower right.



Evaluation of irradiances and heating rates for the broadband (leftmost column of panels) and the 13 narrow longwave bands (other panels) of the limited-area-nwp-narrow-39 CKD model. The black dashed and red solid lines correspond to the average of the 50 profiles for the “present-day” scenario, while the shaded regions encompass 95% of the error.

Model 17: ecCKD limited-area-nwp-narrow-58

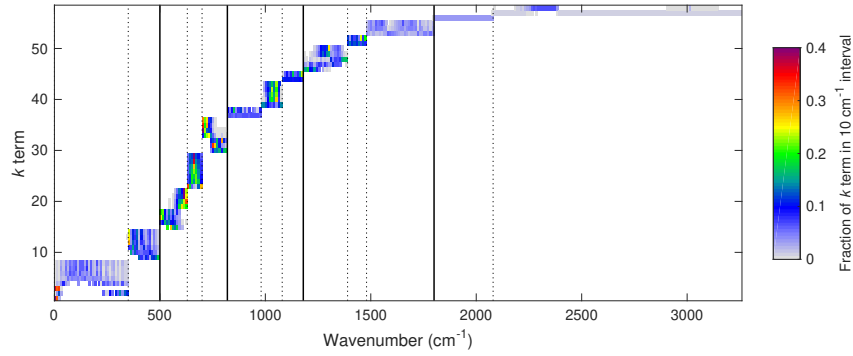
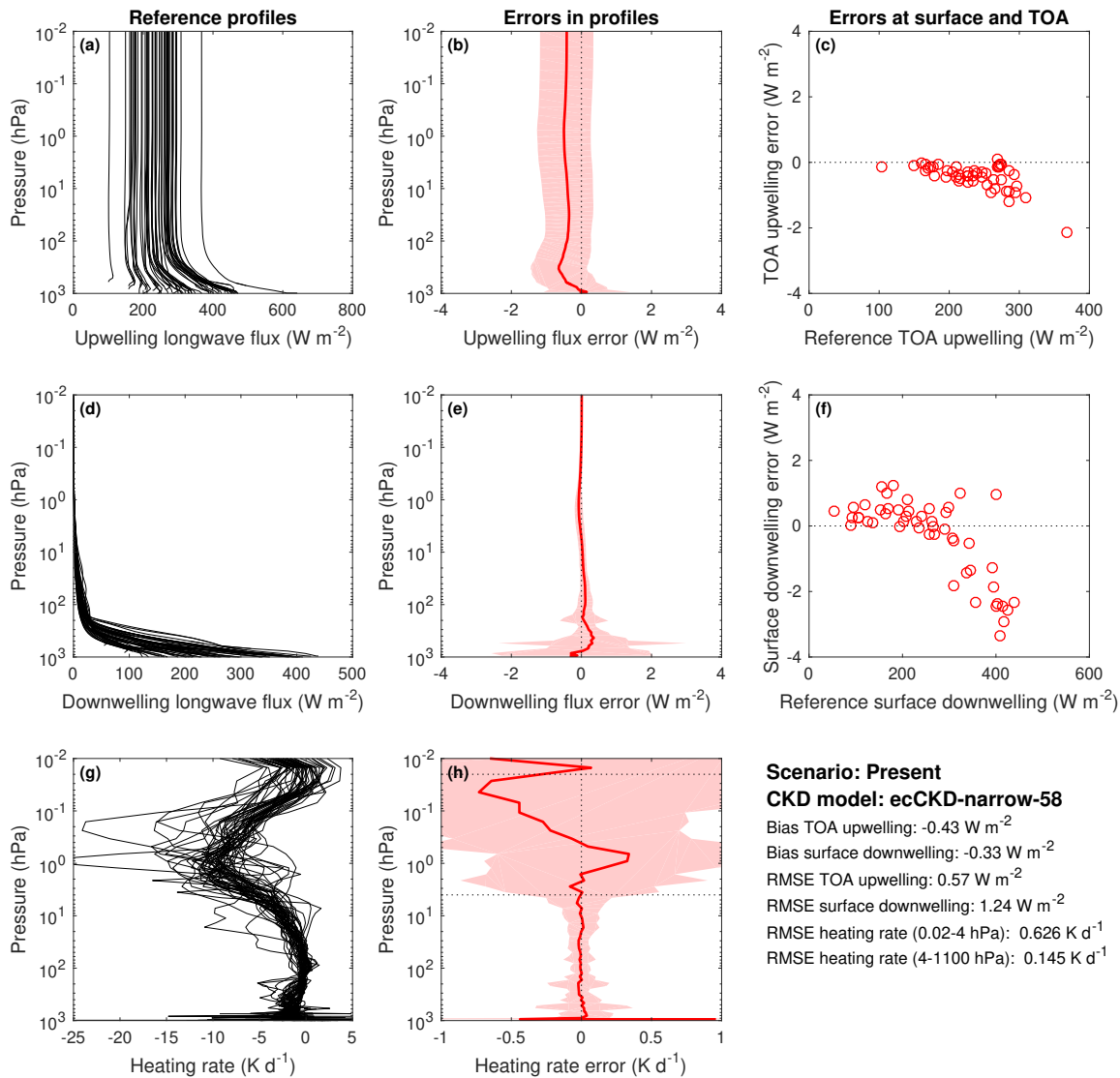
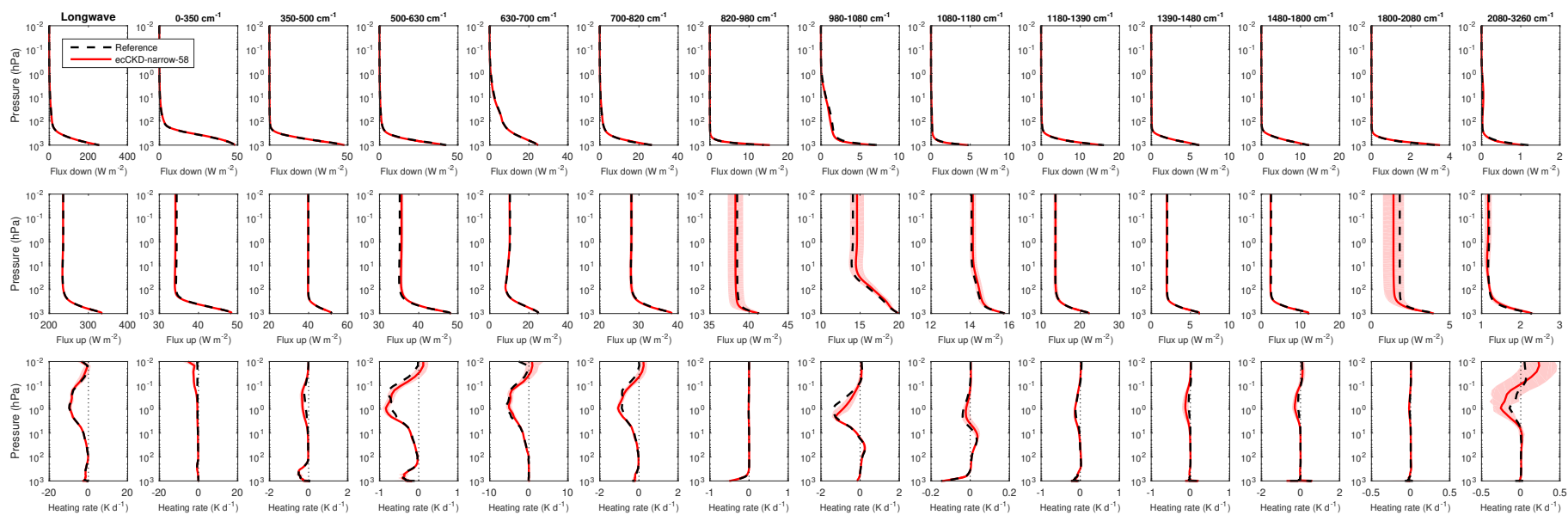


Illustration of the parts of the longwave spectrum that contribute to each k term of the limited-area-nwp-narrow-58 model.



Evaluation of the limited-area-nwp-narrow-58 CKD model for the “present-day” CKDMIP scenario. The left three panels show the irradiances and heating rates from the reference line-by-line calculations. The red lines in the middle three panels show the corresponding bias in these quantities from the CKD model. The shaded regions encompass 95% of the instantaneous errors. Panels c and f depict instantaneous errors in upwelling TOA and downwelling surface irradiances. Error metrics are provided in the lower right.



Evaluation of irradiances and heating rates for the broadband (leftmost column of panels) and the 13 narrow longwave bands (other panels) of the limited-area-nwp-narrow-58 CKD model. The black dashed and red solid lines correspond to the average of the 50 profiles for the “present-day” scenario, while the shaded regions encompass 95% of the error.

Model 18: ecCKD limited-area-nwp-narrow-77

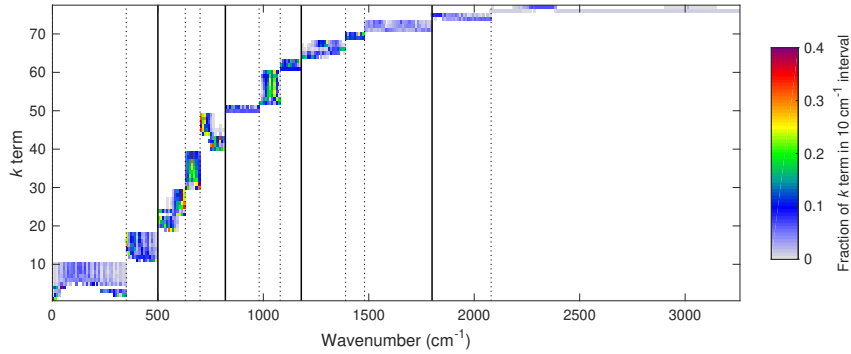
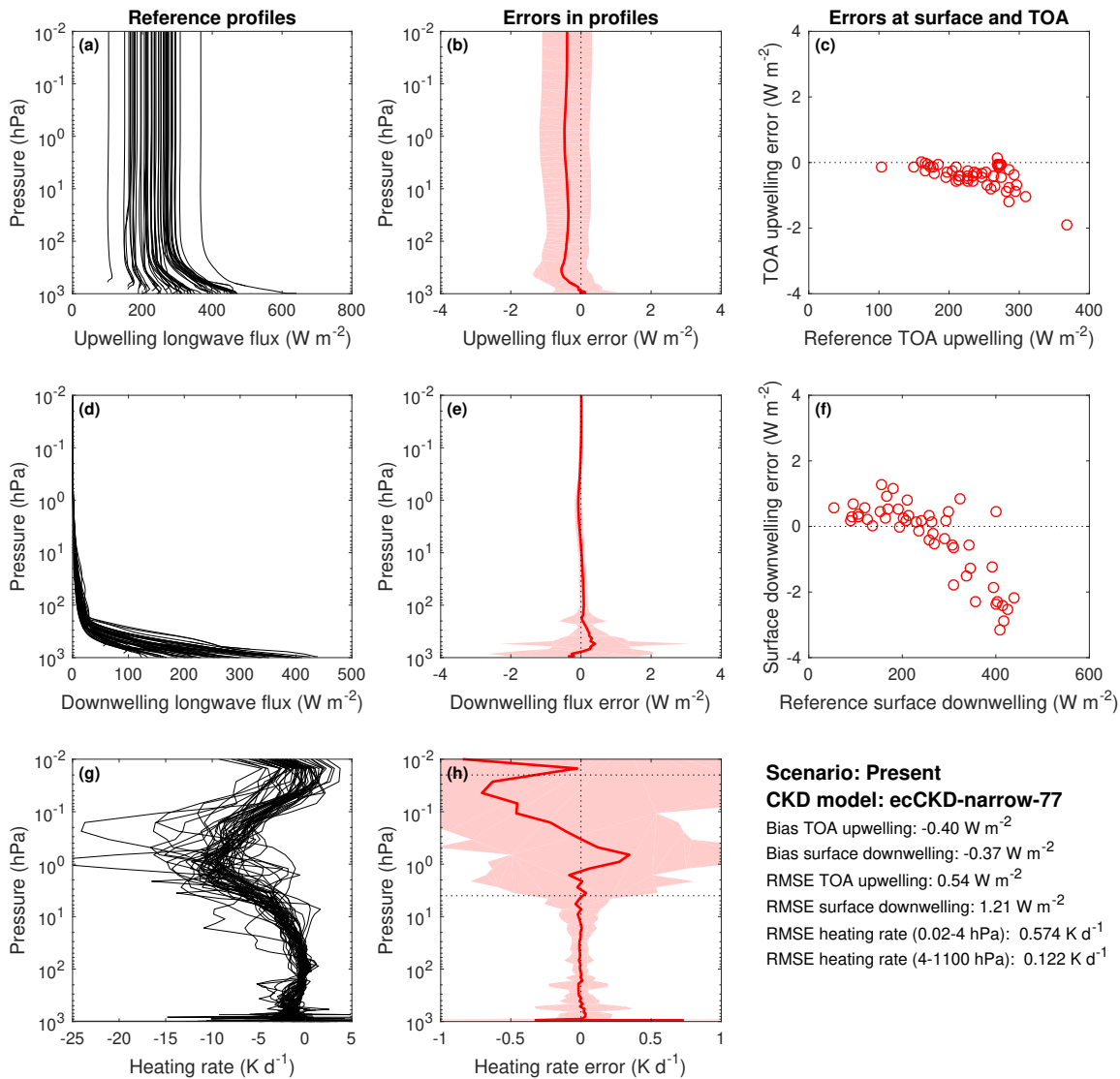
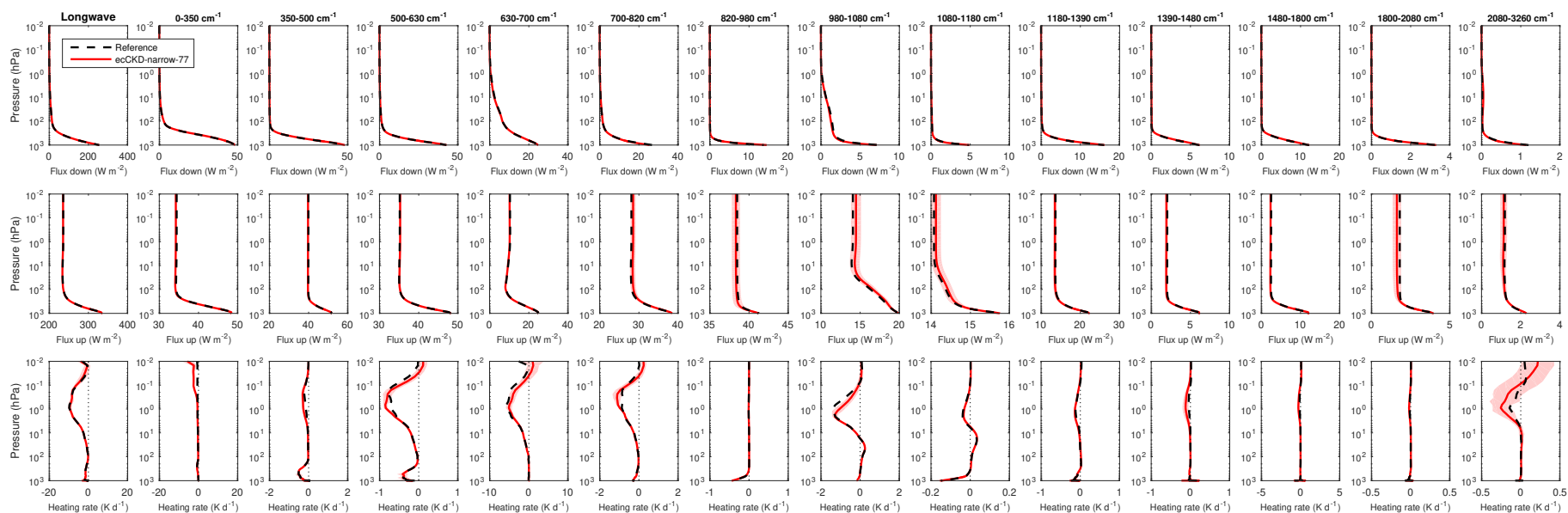


Illustration of the parts of the longwave spectrum that contribute to each k term of the limited-area-nwp-narrow-77 model.



Evaluation of the limited-area-nwp-narrow-77 CKD model for the “present-day” CKDMIP scenario. The left three panels show the irradiances and heating rates from the reference line-by-line calculations. The red lines in the middle three panels show the corresponding bias in these quantities from the CKD model. The shaded regions encompass 95% of the instantaneous errors. Panels c and f depict instantaneous errors in upwelling TOA and downwelling surface irradiances. Error metrics are provided in the lower right.



Evaluation of irradiances and heating rates for the broadband (leftmost column of panels) and the 13 narrow longwave bands (other panels) of the limited-area-nwp-narrow-77 CKD model. The black dashed and red solid lines correspond to the average of the 50 profiles for the “present-day” scenario, while the shaded regions encompass 95% of the error.